Check for updates

Recent progress in cadmium fluorescent and colorimetric probes

Chun-tian Shi, [ab] Zhi-yu Huang,[c] Ai-bin Wu,*[ab] Yan-xiong Hu,[a] Ning-chen Wang,[a] Ying Zhang,[a] Wen-ming Shu [ab] and Wei-chu Yu*[ab]

Cadmium is a heavy metal which exists widely in industrial and agricultural production and can induce a variety of diseases in organisms. Therefore, its detection is of great significance in the fields of biology, environment and medicine. Fluorescent probe has been a powerful tool for cadmium detection because of its convenience, sensitivity, and bioimaging capability. In this paper, we reviewed 98 literatures on cadmium fluorescent sensors reported from 2017 to 2021, classified them according to different fluorophores, elaborated the probe design, application characteristics and recognition mode, summarized and prospected the development of cadmium fluorescent and colorimetric probes. We hope to provide some help for researchers to design cadmium fluorescent probes with higher selectivity, sensitivity and practicability.

School of Chemistry and Environmental Engineering, Yangtze University, Jingzhou, Hubei, People's Republic of China. E-mail: abwu@yangtzeu.edu.cn; yuweichu@126.com

bUnconventional Oil and Gas Collaborative Innovation Center, Yangtze University, Jingzhou, Hubei, People's Republic of China

cKey Laboratory of Textile Fibers and Products, Ministry of Education, College of Materials Science and Engineering, Wuhan Textile University, Wuhan, Hubei, People's Republic of China

1. Introduction

Cadmium, as an essential resource in the earth, is widely used in chemical industry, electronics industry, nuclear industry, semiconducting, quantum dots, phosphate fertilizers, rechargeable batteries, pigments, electroplating, stabilizer, metallurgy, ceramic enamels.[1–6] Consequently, there is a widespread Cd^{2+} contamination in air, water, and soil.[7] Cadmium is a non-essential substance for the organism, and is even classified as a human carcinogen.[8–10] Chronic exposure to Cd^{2+} may cause renal dysfunction, cardiovascular diseases, lung disease, calcium metabolism disorders, eosinophilia, neurodegenerative diseases.[3,11–14] According to World Health Organization (WHO), the permissible concentration of Cd^{2+} in drinking water is 3 μg L^{-1}.[15,16] Therefore, the detection of Cd^{2+} content in organisms, food, and the environment is very important and urgent for life and health.[17,18]

Chun-Tian Shi was born in Yunnan, P. R. China in 1996. She received her B. S. degree from Yunnan Agricultural University in 2019. Then, she entered Yangtze University for her M. A. degree and joined Ai-Bin Wu's research group. She was awarded the excellent graduate student titled by the Graduate School of Yangtze University in 2020. Her research interests focuses on the design, synthesis and application of metal ion-targeted fluorescent probes.

Ai-Bin Wu was born in Hubei, P. R. China in 1973. He received his B. S. degree from Central China Normal University in 1995 and obtained his PhD degree in Applied Chemistry with Dr Xu-Hong Qian from East China University of Science and Technology in 2010. He joined Dr Chang-Guo Zhan's group as a Visiting Scientist at College of Pharmacy, the University of Kentucky. In 2015, he began his independent career as associate professor at School of Chemistry and Environmental Engineering, Yangtze University. His research interests are highly interdisciplinary and include functional dyes, synthesis and application of fine chemicals, medicinal chemistry.

Up to now, there are some traditional detection methods of Cd^{2+} include atomic absorption spectroscopy, ultraviolet-visible spectroscopy, ion selective electrode, inductively coupled plasma mass spectrometry, stripping voltammetry.[19–23] Nevertheless, most of these detection methods require expensive equipment, tedious procedures and skilled operators, and have the characteristics of low detection sensitivity, high economic costs and time-consuming.[18,23–25] By contrast, fluorescent probe detection has the characteristics of strong specificity, high sensitivity, low detection limit, high accuracy, low cost, and visualization, which can replace traditional analysis methods to detect Cd^{2+}.[15,16,26–28] Therefore, the research and application of Cd^{2+} fluorescent sensors is of great interest to many scientific fields, ranging from supramolecular chemistry to life sciences.

Fluorescent sensors consist of fluorophore (signalling) and receptor (guest binding) moieties, either separated by a spacer or integrated into one unit.[29,30] Common fluorophores are rhodamine, naphthalimide, coumarin, quinolone, BODIPY, benzothiazole, fluorescein, diarylethylene.[4,16,17,19,21,22,31–34] Common receptors are pyridine and its analogues, and other structures containing O, N, S and other heteroatoms.[9] According to the generation of fluorescence signals, there are mainly the following mechanisms: photoinduced electron transfer (PET), intramolecular charge transfer (ICT), fluorescence resonance energy transfer (FRET), aggregation-induced emission (AIE), excimer/exciplex formation/extinction, C=N isomerization, excited-state intramolecular proton transfer (ESIPT). In addition, Cd^{2+} fluorescent and colorimetric nanosensors, including metal organic framework (MOF), quantum dots (QDs), nanoclusters (NCs) and nanoparticles (NPs), have also achieved good development in recent years, which makes it more possibilities for the source of raw materials, structural design, recognition methods and application fields of Cd^{2+} probes.

Trace Cd^{2+} is harmful to environment and organism, and the detection of Cd^{2+} ions by fluorescent probes is easily interfered by other transition metals, especially Zn^{2+} ions in the same

group.[3,21] Therefore, the development of Cd^{2+} fluorescent probes has great challenges and significance for the detection of Cd^{2+} in environment and living organisms. At present, a plethora of fluorescent probes for Cd^{2+} have been reported and this research field has become very active. A closer scrutiny of the review literatures on the research progress of Cd^{2+} fluorescent probes in the web of science core collection shows that J. Jia et al. reviewed Zn^{2+}/Cd^{2+} fluorescent probes based on small organic molecules in 2012, and S. Y. Chen et al. reviewed $Pb^{2+}/Cd^{2+}/Hg^{2+}$ fluorescent probes based on small organic molecules in 2021.[35,36] Apart from these, there is no relevant or targeted review article that has covered research advances of Cd^{2+} fluorescent probes. Therefore, as a review article dedicated to the research progress of Cd^{2+} fluorescent probes, this article adopts a classification method different from the above reviews. Since the mechanism of some fluorescence response is inferred by the authors and has not been demonstrated absolutely, and there may be two or more possible mechanisms might simultaneously exist in the sensing process, we described the probes based on the category of fluorophore species. It should be noted that this article elaborated and summarized the Cd^{2+} ion fluorescent probes reported in recent years in terms of the probe design ideas, application characteristics, and binding methods, and discussed the reality and future challenges of Cd^{2+} ion fluorescent probes used in environmental monitoring and biological imaging.

2. Quinolone-based Cd^{2+} fluorescent sensor

Quinoline is a kind of fluorescent chromophore with coordination function, recognition function, strong photostability and metal ion chelating ability.[9] The conjugated system of quinoline is large and prone to $\pi–\pi^*$ electronic transition. Its own N atom easily forms hydrogen bonds in polar solvents and exhibits weak fluorescence. After complexing with metal ions, the fluorescence recovers.

2.1 Quinolone as a binding site for Cd^{2+}

Y. Mikata's team reported on a series of fluorescent probes (Fig. 1) for detecting Cd^{2+}, and quinoline chromophores in these probes can also be used as binding sites.[1,37,38] In 2017, they synthesized probe 1a and its thia (1b) and aza (1c) derivatives.[1] In DMF–H_2O (1 : 1) solution and an excitation at 317 nm, the probes 1a, 1b and 1c exhibit weak fluorescence. The binding of the probes to Cd^{2+} inhibits their PET process and make the adjacent quinoline rings in the probes formed an intramolecular excimer, so these probes exhibit enhanced fluorescence emission. The detection limit of probe 1a for Cd^{2+} is 22 nM. The dissociation constant of the complexes of probe 1a, 1b, 1c and Cd^{2+} were $(4.2 \pm 0.7) \times 10^{-7}$ M, $(6.5 \pm 0.2) \times 10^{-6}$ M and $<2 \times 10^{-7}$ M, respectively. The O in probe 1a is replaced by S and N can increase the selectivity of Cd^{2+}. For the detection of Cd^{2+} by these probes, although the fluorescence response interference caused by Zn^{2+} can be neglected, the presence of

Wei-Chu Yu was selected as the National "Hundred, Thousand, Ten Thousand" talent project candidate in 2014 and the distinguished professor at Yangtze University. He attended China University of Petroleum (Beijing) to receive his PhD degree in 2006. After that he performed postdoctoral research at China University of Petroleum (Beijing) under the direction of Dr Chang-Ming Su, he joined Dr Yong-Chun Tang's and Ce Liu's group as senior Visiting Scientist at California Energy Research Institute and University of Houston, respectively. Prof. Yu's research involves the synthesis and application of fine chemicals, especially in applied chemistry of oil and gas fields.
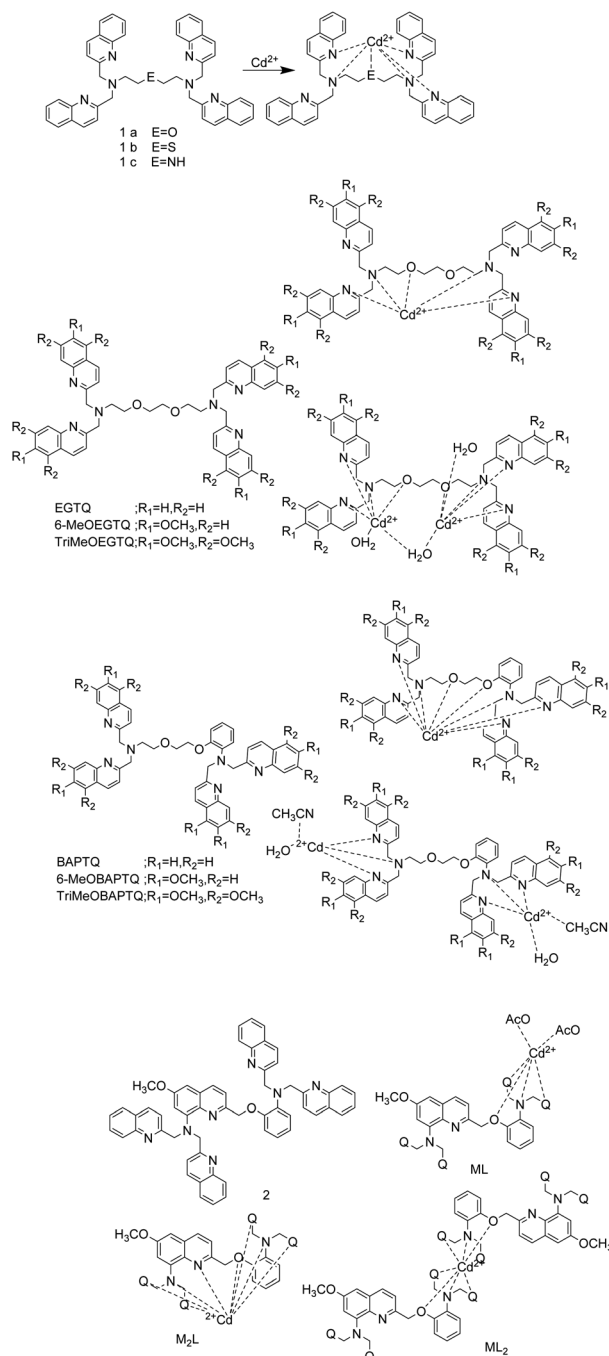
Fig. 1 The probes structure reported by Y. Mikata's team and proposed binding mode with Cd^{2+}.

Cu^{2+}, Ag^+, Hg^{2+}, Cr^{3+} and Fe^{3+} in the detection system can interfere with the fluorescence signal obviously.

In 2019, they designed methoxy-substituted tetrakisquinoline **EGTA** and **BAPTA** analogs probes that can recognize Cd^{2+} based on PET mechanism.[37] All **EGTQ** derivatives bind to Zn^{2+}, Cd^{2+}, Fe^{3+}, Co^{2+}, Hg^{2+} and Ag^+ as indicated by the UV-vis spectral changes. However, only Zn^{2+} and Cd^{2+} can illuminate the ligand. Although they selectivity is poor, methoxy substitution can enhance the selectivity to Cd^{2+} to some extent. **TriMeO-BAPTQ** probe was synthesized by introducing three methoxy

groups at positions 5, 6, and 7 of each quinoline moiety in **BAPTQ**. In methanol–HEPES buffer (9 : 1, 50 mM HEPES, 0.1 M KCl, pH = 7.5), upon excitation at 347 nm, **TriMeOBAPTQ** can combine with Cd^{2+} in a stoichiometric ratio of 1 : 1 or 1 : 2 to increase the fluorescence of the system, and detect Cd^{2+} as low as 9.9 nM. **TriMeOBAPTQ** also has affinity with Cu^{2+}, Ag^+, Hg^{2+}, and Fe^{3+}, even the presence of a large number of these metal ions except Cu^{2+} does not affect the detection of Cd^{2+} by **Tri-MeOBAPTQ** probe.

To improve the metal ion specificity and sensitivity, they changed core structure from **BAPTA** to Ca^{2+}-specific probe (quin2(8-amino-2-((2-amino-5-methylphenoxy)methyl)-6-methoxyquinoline-N,N,N',N'-tetraacetic acid)) to synthesize probe **2**, and reported it in 2020.[38] Probe **2** has two chromophores, methoxy-substituted and unsubstituted quinolines. Because the aqueous solvent prevents the probe **2** from coordinating with metal ions, the test was carried out in methanol solution. The combination of probe **2** and Cd^{2+} can inhibit the PET process and produce CHEF (chelation-enhanced fluorescence) and excimer effects when excited by 317 nm light, which increased the fluorescence intensity of the probe **2** by 170 times at 408 nm. The detection limit of probe **2** for Cd^{2+} is 182 nM. The equimolar amounts of Co^{2+} and Ag^+ shut down the Cd^{2+}-induced fluorescence, and the excessive Zn^{2+} and Ni^{2+} can replace Cd^{2+} to bind to probe **2**. Although the probe has enhanced fluorescence and specific selection for Cd^{2+} by introducing 6-methoxy-8-aminoquioline moiety, the sensor still has weak water solubility, low selectivity, and short excitation and emission wavelengths. Moreover, the detection of low concentrations of Cd^{2+} should prevent weak fluorescent ML_2 is generated. Y. Mikata *et al.* proposed to introduce a suitable electron-donating substituents on the side-arm quinolones, which act as a metal binding site and chromophore to improve sensor performance.[38]

In 2017, the sulfonamidoquinoline-based derivatives sensor **3** (Fig. 2) was reported by Y. Zhang *et al.*[39] In DMSO–water (3 : 2 (v/v), 0.01 M Tris–HCl, pH = 7.24) solution, sensor **3** and Zn^{2+}/Cd^{2+}/Hg^{2+} are combined in a mole ratio of 2 : 1 to red-shift the absorption maximum from 323 nm to 425/422/424 nm. When excited at 422 nm, the detection system including sensor **3** and Zn^{2+}/Cd^{2+}/Hg^{2+} emits red fluorescence at 634/618/630 nm, with an intensity increase of 38/96/21 times. In addition, the fluorescence intensity is linearly related to the concentration of Zn^{2+}/Cd^{2+}/Hg^{2+}. The detection limit of sensor **3** to Zn^{2+} is 3.61 nM, to Cd^{2+} is 1.55 nM, and to Hg^{2+} is 7.02 nM, which is lower than the permissible concentrations of Cd^{2+} (43.8 nM) and Hg^{2+} (9.9 nM) in drinking water regulated by Environmental Protection Agency (EPA). The binding constants ($\log K_s$) decreased with the increase of ion radius in group IIB, and the binding constants of Zn^{2+}, Cd^{2+} and Hg^{2+} and sensor **3** were 9.45, 9.36 and 8.96, respectively. The sensor **3** can detect Zn^{2+}, Cd^{2+} and Hg^{2+} in the aqueous solution under the excitation of visible light. In addition, the sensor **3** was used for Cd^{2+} competition experiments and fluorescence imaging in yeast cells, indicating that the sensor **3** is biocompatible and not affected by metal ions except Zn^{2+} and Cu^{2+} in the fluorescence detection of Cd^{2+}.
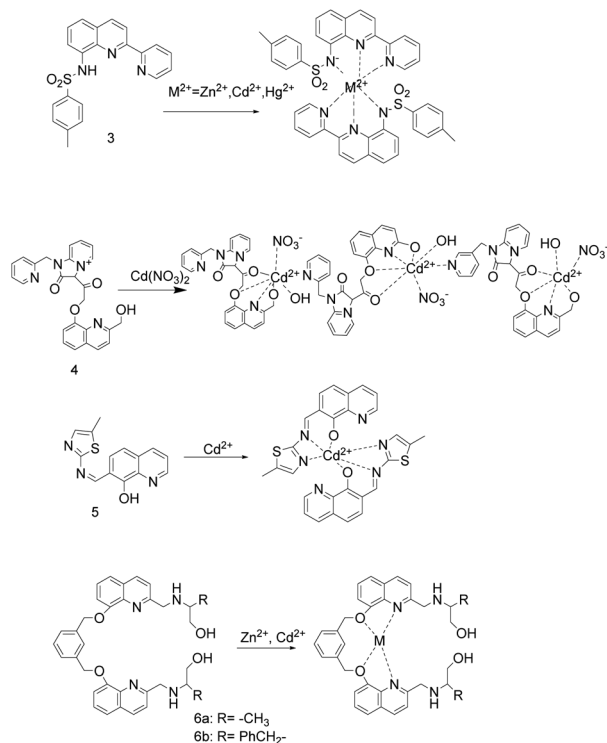
Fig. 2 Proposed binding mode of probes 3 to 6 with Cd^{2+}.

Y. P. Dai and coworkers described probe 4 (Fig. 2).[9] In Tris–HCl buffer (10 mM, pH = 7.4), the detection limit to Cd^{2+} is 1.18 $\times 10^{-6}$ M and the association constants is 9.00×10^4 M^{-1}. Upon excitation at 312 nm, probe 4 has weak fluorescence due to the double PET process from the oxygen atom of hydroxy to hydroxyquinoline group and the hydroxyquinoline to carbonyl unit, respectively. After the chelation of probe 4 with Cd^{2+}, the PET process was inhibited, causing the fluorescence of probe 4 emission peak to redshift from 400 nm to 410 nm and the fluorescence to increase by 2.5 times. Although probe 4 is almost 100% soluble in water, reversibility, non-toxic and cell-membrane-permeable, the presence of Fe^{3+}, Fe^{2+}, Cu^{2+}, Cr^{3+}, Al^{3+} or Ag^+ ions can quench part of the fluorescence enhancement caused by Cd^{2+} to some extent. At 410 nm, the fluorescence intensity of the Cd^{2+} complex probe 4 is very little affected by other metal ions, but Fe^{3+} can partially quench the fluorescence.

X. H. Ding's research group reported sensor 5 (Fig. 2).[40] In CH_3CN/H_2O (1 : 1) systems, sensor 5 combined with Cd^{2+} made the solution turn dark yellow immediately, and turn blue fluorescence under 365 nm UV light. The association constant of sensor 5 and Cd^{2+} is estimated to be 8.48×10^4 M^{-1}. In the pH range of 6–10, sensor 5 has high selectivity, anti-interference ability and bioimaging ability. It can detect Cd^{2+} as low as 4×10^{-6} mol L^{-1} and not be interfered by other cations. In addition, the complex of sensor 5 and Cd^{2+} can be used as a highly selective and sensitive probe for PO_4^{3-} without interference from anions.

In 2017, X. Y. Liu's team reported two turn-on fluorescent sensors 6a and 6b (Fig. 2) for Zn^{2+}/Cd^{2+}, and their complexes can act as highly selective sensors to detect phosphate anion through turn-off the fluorescence.[11] In CH_3OH/H_2O (1 : 1, v/v, Tris 10 mol L^{-1}, pH = 7.4) solution, upon the excitation at 310 nm, sensor 6a/6b has weak fluorescence. Adding Zn^{2+}/Cd^{2+} into the sensor solution, an obvious fluorescence turn-on response at 430 nm, and a working curve can be established between the fluorescence intensity and the concentration. The binding constants of sensors 6a and 6b to Zn^{2+} or Cd^{2+} are $(1.517 \pm 0.31) \times 10^7$, $(6.40 \pm 0.15) \times 10^6$, $(9.16 \pm 0.42) \times 10^5$, and $(1.03 \pm 0.19) \times 10^6$ L mol^{-1}, respectively. Adding anion into the complexes of sensor 6a/6b and Zn^{2+}/Cd^{2+}, and it is found that $H_2PO_4^-$ and HPO_4^{2-} can almost quench all fluorescence. However, the article does not specifically describe the distinction between Zn^{2+} and Cd^{2+}, $H_2PO_4^-$ and HPO_4^{2-}.

In 2019, H. H. Song's research group synthesized probe 7 (Fig. 3) by inserting an amide group into the 8-aminoquinoline fluorophore and a propargylamine chelating site.[41] Probe 7 displayed selective and distinct ratiometric fluorescence response to Zn^{2+} and Cd^{2+}, Zn^{2+} was bound as an amide tautomer in almost totally water solution, and Cd^{2+} was bound as an imidic acid tautomer in CH_3CN aqueous medium, respectively. Under 365 nm light, in the high/low acetonitrile content aqueous solution, probe 7 and Cd^{2+}/Zn^{2+} combined 1 : 1, making probe 7 emitted bright-green/green fluorescence and the emission peak is red-shifted 95/82 nm. The fluorescence intensity ratios of $I_{500 \text{ nm}}/I_{405 \text{ nm}}$ and $I_{498 \text{ nm}}/I_{416 \text{ nm}}$ were linearly proportional to the concentration of Cd^{2+} and Zn^{2+}, respectively. The association constants of probe 7 with Cd^{2+} and Zn^{2+} are is 3.7×10^4 M^{-1} and 1.4×10^4 M^{-1}, respectively. The detection limits for Cd^{2+} is 0.055 μM and for Zn^{2+} is 0.063 μM. The response of probe 7 to Zn^{2+} and Cd^{2+} is selective, reversible, and rapid. The coexistence Cu^{2+}, Ni^{2+}, Co^{2+} with Cd^{2+} quenched the Cd^{2+}-induced fluorescence, while the coexistence Cr^{3+} with Zn^{2+} slightly quenched the Zn^{2+}-induced fluorescence. Probe 7
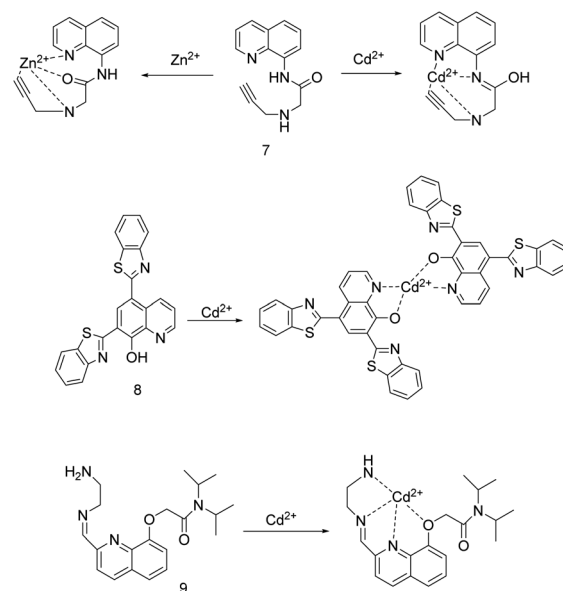

Fig. 3 Proposed binding mode of probes 7 to 9 with Cd^{2+}.

was applied for detecting analysis of all the target ions in the tap water sample and on test paper strips, and bioimaging of Zn^{2+} in mung bean sprouts as well. In addition, the complex of probe 7 and Zn^{2+} can be used as a secondary sensor for PPi and ATP.

The same year, Z. N. Lu *et al.* synthesized 8-hydroxyquinoline-benzothiazole conjugated probe 8 (Fig. 3) in two steps.[42] This probe can greatly enhance the fluorescence by coordinating with various metal ions such as Al^{3+}, Cd^{2+}, Zn^{2+}, Mg^{2+} in methanol containing 1% water. However, the selectivity to Cd^{2+} can be achieved by increasing the water content to 30% aqueous methanol solution. The aqueous methanol solution (pH = 7.4, 30% Tris–HCl buffer) and the excitation at 313 nm are selected to carry out. Probe 8 and Cd^{2+} combined at a 2 : 1 stoichiometry between probe 8 and Cd^{2+} to emit green fluorescence, and the fluorescence intensity at 525 nm had a good linear relationship with the concentration of Cd^{2+} over a range of 0–5 μM. The detection limit for Cd^{2+} is 0.1 μM. Adding EDTA as a competing chelator can make the binding of probe 8 and Cd^{2+} reversible. Probe 8 can detect Cd^{2+} in an aqueous solution with a pH of 4–12, and be used for fluorescence imaging of Cd^{2+} in living cells.

The group headed by X. J. Wan described a quinoline Schiff base-containing sensor 9 (Fig. 3).[33] After optimizing the detection environment, the researchers found that the better selectivity and sensitivity of the probe to Cd^{2+} under the conditions of pH = 4 methanol solution (10%) and excitation wavelength of 246 ± 2 nm. The combination of non-fluorescent sensor 9 and Cd^{2+} caused sensor 9 to turn on the fluorescence response at 425 nm. At this time, sensor 9 displayed excellent selectivity, sensitivity, and reversibility for detecting Cd^{2+} in an acidic environment, and it can detect Cd^{2+} as low as 2.4 nM.

In 2019, K. Aich and colleagues reported on quinoline–benzothiazole-based fluorescent turn-on probes 10 and 11 (Fig. 4).[43] In MeOH/H_2O (3/7, v/v, 10 mM HEPES buffer, pH = 7.2) solution, upon the excitation at 360 nm, the fluorescence emission intensity of probes 10 and 11 are linearly related to the concentration of Cd^{2+}. Their detection limits for Cd^{2+} are 3.52×10^{-10} M and 4.83×10^{-9} M, respectively, and the association constants are 3.17×10^4 M^{-1} and 1.60×10^4 M^{-1}, respectively. Because the nitrogen atoms of quinoline and pyridine are strongly coordinated with Cd^{2+}, the ICT effect of the probes is enhanced. The fluorescence emission of probe 10 is red-shifted from 488 nm to 507 nm and the fluorescence is changed from weak cyan to green. The fluorescence emission of probe 11 is

increased by 20 times, the fluorescence emission is red-shifted from 490 nm to 510 nm and the fluorescence is changed from cyan to bright green. Probe 10 and probe 11 have high selectivity and reversibility (Na_2EDTA) for Cd^{2+} detection, and are not interfered by other metal ions, and can act as a potential portable kit for detection of Cd^{2+} in solid state as well as in solution.

The next year, S. Nazerdeylami *et al.* described probe 12 (Fig. 4), which is effective for detecting Cd^{2+} and tetracycline.[44] The 8-hydroxyquinoline dehydrogenation is connected to β-cyclodextrin, which increases the rigidity of the probe 12. In an aqueous medium, upon excitation at 350 nm, probe 12 has a strong fluorescence emission intensity at 525 nm. The N in the pyridine ring and the O in the chelator interacted with Cd^{2+}, causing the fluorescence of the probe 12 to be quenched. The fluorescence intensity is linearly related to the Cd^{2+} content of 0.1–1.5 nM. At pH < 4, the solution hydrates H^+ ions due to the protonation of nitrogen and oxygen, causing H^+ and other metal ions to compete chelating sites. At pH > 4, cadmium hydroxide precipitates is formed. Therefore, the probe 12 is suitable for detecting Cd^{2+} in an aqueous medium with pH = 4, and the detection has selectivity, sensitivity, and anti-interference. The detection limit of probe 12 for Cd^{2+} is 0.05 nM. Further, the complex of probe 12 and Cd^{2+} can be used as a fluorescence-on probe of tetracycline, the fluorescence intensity is linearly related to the content of tetracycline, and can detect tetracycline as low as 0.9 μM.

S. L. Li *et al.* Reported the probe 13 (Fig. 5) responding to Ag^+ (PET) and Cd^{2+} (ICT) based on different mechanisms.[45] In the CH_3OH/HEPES (9 : 1, v/v, pH = 7.30) buffer system and the excitation wavelength of 344 nm, the fluorescence of the probe was quenched by 88% with the addition of Ag^+ and showed an "on–off" behavior. With the addition of Cd^{2+}, the maximum fluorescence emission of the probe was red shifted from 465 nm to 490 nm, the fluorescence intensity was quenched by 33%, and the fluorescence changed from blue to green. The recognition of Cd^{2+} is not affected by metal ions including Ag^+, while the recognition of Ag^+ ions is interfered by other metal ions. The selectivity and sensitivity of the probe for Cd^{2+} ion are stronger than that for Ag^+. The complexation constant of the probe for Cd^{2+} is 2.23×10^4 M^{-1}, and the detection limit for Cd^{2+} is 0.26 mM. The complex of probe 13 and Cd^{2+} could be used for sequential recognition of S^{2-}. When Cd^{2+} and S^{2-} were added alternately for 3 times, the probe still had a high level of recognition ability. Under strong acidic or alkaline conditions, probe 13 may change its own structure or lose the ability of ion coordination and cannot recognize ions.
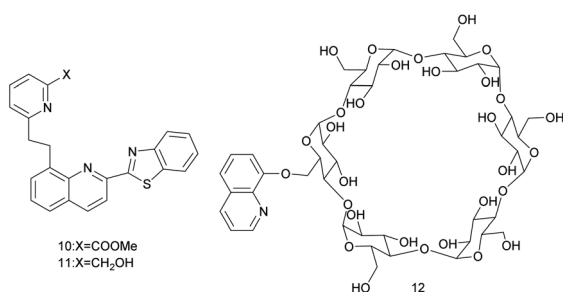

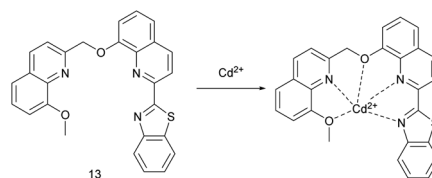**Fig. 4** The structure of probes 10 to 12.

Fig. 5 Proposed binding mode of probe 13 with Cd^{2+}.

2.2 Quinolone does not as a binding site for Cd²⁺

In 2017, the first metal ion sensor **14** (Fig. 6) of 4,5-quinolinimide derivatives was synthesized by Y. Zhang *et al.*[7] To increase the selectivity of 2,2-dipicolylamine (DPA) for Cd^{2+} over the same group element Zn^{2+}, an amide group was introduced into the DPA unit. In a methanol–water (1 : 1) solution with a pH of 7.20, upon excitation at 430 nm, adding Cd^{2+} increased the fluorescence of sensor **14**, and the fluorescence intensity was linearly related to the concentration of Cd^{2+}. The complex's association constant is 9.06×10^7 M⁻¹. The detection limit of sensor **14** for Cd^{2+} is 11 nM, which is lower than the permissible concentration of Cd^{2+} in drinking water regulated by the World Health Organization as 26 nM. The fluorescence emission of sensor **14** binding to Zn^{2+} is weaker and the fluorescent lifetime is shorter, which makes it possible to distinguish between Zn^{2+} and Cd^{2+}. Under physiological conditions, the fluorescence of sensor **14** binding to Cd^{2+} can be significantly quenched by Cu^{2+}. In addition, sensor **14** has low cytotoxicity and emits bright yellow-green fluorescence when used to fluorescence imaging of Cd^{2+} in yeast cells.

In 2019, P. G. Mahajan's team reported the Schiff base probe **15** (Fig. 6).[6] The probe can quickly detect Cd^{2+}, Co^{2+}, Ni^{2+}, Cu^{2+} in nano-molar level through absorption or fluorescence spectroscopy. Adding Cd^{2+}, Ni^{2+}, Cu^{2+}, Co^{2+} to the systems of methanol : water (7 : 3, v/v) and probe **15** for 3–5 minutes causes the probe solution to change from colorless to pale yellow, yellow, yellow, and dark yellow, and the absorption peaks red-shifts from 338 nm to 399 nm, 422 nm, 424 nm, 396 nm, respectively. The detection limits of probe **15** for Cd^{2+} is 1.043 nM, for Ni^{2+} is 0.656 nM, for Cu^{2+} is 0.224 nM, for Co^{2+} is 1.047 nM. Upon excitation at 340 nm, the complex of probe **15**

with Cd^{2+}, Ni^{2+}, Co^{2+}, Cu^{2+} absorb the energy from light followed by immediately return to ground state without photon emission, resulting in fluorescence quenching by 8.1, 9.2, 8.6, 10.5 times, respectively. The detection limits are 1.070 nM for Cd^{2+}, 0.637 nM for Ni^{2+}, 1.053 nM for Co^{2+}, and 0.184 nM for Cu^{2+}. In the aqueous solution with a pH of 6–8, and the affinity of probe **15** for metal ions is $Cd^{2+} < Co^{2+} < Ni^{2+} < Cu^{2+}$, and the metal ions with strong affinity can replace metal ions with weak affinity to bind the probe **15**.

Y. Xiao *et al.* designed the probe **16** (Fig. 6) by connecting quinoline fluorophore with tripyridine recognition group.[46] Due to the strong absorption at 470 nm and the elimination of the interference of the original fluorescence in DMF–H₂O (FW 40% v/v) solution, they were selected as the conditions for the study of the probe recognition performance. At 520 nm, there was a good linear relationship between the fluorescence emission intensity and the concentration of Cd^{2+} (0–5 μmol L⁻¹) and Zn^{2+} (6–10 μmol L⁻¹). The LOD of this fluorescent probe **16** for Cd^{2+} is 3.5×10^{-8} mol L⁻¹. However, the presence of Zn^{2+} and Cu^{2+} affects the recognition of Cd^{2+} by the probe. Because the fluorescence of this probe induced by Zn^{2+} is stronger than that induced by Cd^{2+}, the binding of Cu^{2+} to the probe is more stable and can quench the fluorescence induced by Cd^{2+}.

A. Garau *et al.* synthesized probe **17** (Fig. 6) by inserting amide group spacer between quinoline fluorophore and 1-aza-4,7,10-trithiacyclododecane ([12]aneNS₃) receptor unit.[47] In MeCN/H₂O (1 : 4, v/v) solution, the probe showed fluorescence enhancement in response to Cd^{2+} and Zn^{2+} due to CHEF effect, and Cd^{2+} induced fluorescence enhancement was stronger than that caused by Zn^{2+}.

2.3 Binding mode remains unknown

In 2018, an "on–off–on" sensor **18** (Fig. 7) for sequential recognition of Cu^{2+} and Cd^{2+} reported by J. Han *et al.*[48] In EtOH/H₂O (v/v = 1 : 9) solution, sensor **18** emits strong blue fluorescence at 471 nm (the excitation at 340 nm), adding Cd^{2+} decreased the fluorescence intensity and red-shifted 40 nm, and the fluorescence changed from blue to green. Cu^{2+} binds to sensor **18** at a ratio of 1 : 1, quenching the blue fluorescence of sensor **18**. The detection limit for Cu^{2+} is 2.7×10^{-8} M, and the association constant is 5.643×10^4 M⁻¹. The complex of sensor **18** and Cu^{2+} can be replaced by Cd^{2+} and emerge a strong emission peak at 510 nm to become a more sensitive and accurate fluorescent probe of Cd^{2+}, which significantly increases the fluorescence intensity of the system. The complex
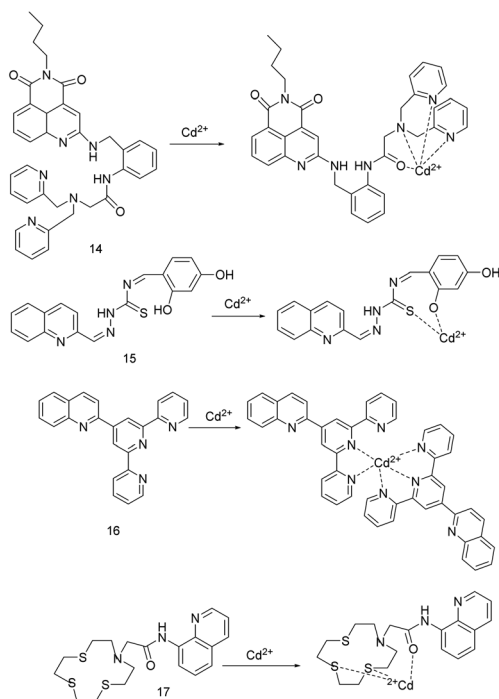

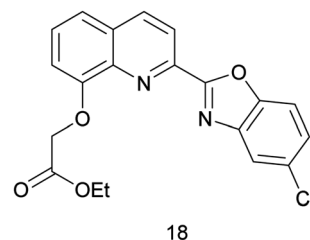**Fig. 6** Proposed binding mode of probes **14** to **17** with Cd²⁺.

Fig. 7 The structure of probe **18**.

Table 1 Spectroscopic and analytical parameters of the quinolone-based Cd^{2+} fluorescent probes

Probe	Solvent	Excitation wavelength (nm)	Emission wavelength (nm) $\lambda_{em_0}-\lambda_{em}$	Detection limit (nM)	Association constant (M^{-1})	Interfering ion(s)	Ref.
1a	$DMF–H_2O$ (1 : 1)	317	428	22	$K_d = (4.2 \pm 0.7) \times 10^{-7}$ M	Cu^{2+}, Ag^+, Hg^{2+}, Cr^{3+}	1
TriMeO-BAPTQ	$CH_3OH–H_2O$ (9 : 1)	347	460	9.9	—	Cu^{2+}	37
2	CH_3OH	317	408	182	—	Co^{2+}, Ag^+, Zn^{2+}, Ni^{2+}	38
3	$DMSO–H_2O$ (3 : 2)	422	618	1.55	$\log K_s = 9.36$	Zn^{2+}, Cu^{2+}	39
4	H_2O	312	410	1180	9.00×10^4	Fe^{3+}	9
5	$CH_3CN–H_2O$ (1 : 1)	375	500	4000	8.48×10^4	PO_4^{3-}	40
6a/6b	$CH_3OH–H_2O$ (1 : 1)	310	430	—	$(1.517 \pm 0.31) \times 10^7 /$ $(1.03 \pm 0.19) \times 10^6$	Zn^{2+}, $H_2PO_4^-$, HPO_4^{2-}	11
7	$CH_3CN–H_2O$	321	405–500	55	3.7×10^4	Cu^{2+}, Ni^{2+}, Co^{2+}	41
8	$CH_3OH–H_2O$ (7 : 3)	313	525	100	—	—	42
9	$CH_3OH–H_2O$ (1 : 9)	246	425	2.4	—	—	33
10	$CH_3OH–H_2O$ (3 : 7)	360	488–507	0.352	3.17×10^4	—	43
11	$CH_3OH–H_2O$ (3 : 7)	360	490–510	4.83	1.60×10^4	—	43
12	H_2O	350	525	0.05	—	Tetracycline	44
13	$CH_3OH–H_2O$ (9 : 1)	344	465–490	260 000	2.23×10^4	—	45
14	$CH_3OH–H_2O$ (1 : 1)	430	543	11	9.06×10^7	Cu^{2+}, Zn^{2+}	7
15	$CH_3OH–H_2O$ (7 : 3)	340	About 420	1.070	6.73×10^5	Co^{2+}, Ni^{2+}, Cu^{2+}	6
16	$DMF–H_2O$ (6 : 4)	470	520	35	—	Zn^{2+} and Cu^{2+}	46
17	$MeCN–H_2O$ (1 : 4)	330	505	—	—	Zn^{2+}	12
18-Cu	$EtOH/H_2O$ (1 : 9)	340	510	17	1.374×10^4	—	48

of sensor **18**-Cu can detect Cd^{2+} as low as 1.7×10^{-8} M, and the association constant is 1.374×10^4 M^{-1}. Sensor **18** is stable in the pH range from 4 to 10, and can successively quantitatively detect Cu^{2+} and Cd^{2+} in real water samples and deproteinized milk. Test strips containing sensor **18** also has a good qualitative recognition performance for target ions.

Among the Cd^{2+} fluorescent probes reported in recent five years, the research quinolone-based sensors is the most, and the spectroscopic and analytical parameters of these probes are shown in Table 1. Quinoline is widely used in the design of Cd^{2+} fluorescent probes because it can not only be used as fluorescent chromophore, but also as Cd^{2+} binding site. However, most of these sensors have some problems, such as poor water solubility, poor selectivity, poor anti-interference, short excitation and emission wavelength, which greatly limits their application in the fields of environment and biology. Compared with other sensors, sensors **9** and **18**-Cu have higher selectivity, sensitivity and anti-interference ability. However, the optimum test condition of sensor **9** is pH = 4, which is not suitable for the application in real environment. The sensor **18**-Cu responds to Cd^{2+} by replacing Cu^{2+} with Cd^{2+}, which makes the detection of Cd^{2+} more accurate. It is not be limited to the small molecule probe directly used for Cd^{2+} detection, therefore, it can also be used for Cd^{2+} detection after the probe is complexed with other analytes in the future.

3. Coumarin-based Cd^{2+} fluorescent sensor

Coumarins are characterized by high molar extinction coefficient, high fluorescence quantum yield, large stokes shift, low toxicity, good water solubility and many reaction sites. In addition, coumarin is easy to connect to different groups, and

can not only act as a fluorescent chromophore, but also as recognition sites of analytes, so as to achieve fluorescence response to different analytes.[34,49]

3.1 Coumarin as a binding site for Cd^{2+}

In 2017, C. Kumari's research team synthesized probe **19** (Fig. 8), which recognizes Cd^{2+} and turns on fluorescence.[2] There is a spectral overlap between the energy donor coumarin part and the energy acceptor rhodamine part, and Cd^{2+} is recognized based on the FRET mechanism. In methanol/water (2/1, v/v, 1 mM HEPES buffer, pH = 7.2), the free probe has no characteristic absorption peak in the visible light region, but the absorption peak intensity at 561 nm is increased after gradually adding Cd^{2+}. Upon the addition of Cd^{2+}, the probe **19** and Cd^{2+} are combined in a ratio of 1 : 1 to open the spirolactam ring. The solution immediately changed from colorless to pink, turned non-fluorescent to bright red fluorescent under long wavelength UV light, and shifted the fluorescence emission peak from 430 nm to 589 nm (the excitation wavelength at 340 nm). The binding constant value of the probe to Cd^{2+} was 7.8×10^5 M^{-3} and the detection level was 10.1 nM. Probe **19** can detect Cd^{2+} in a semi-aqueous environment with a pH of 1.0–11.0, with excellent selectivity and sensitivity, and is not interfered by other metal ions. Further, bio-imaging study and cytotoxicity test confirm that it can be used for detecting Cd^{2+} in living HeLa S3 cells.

In 2017, Shaily et al. synthesized the coumarin-chalcone conjugated probe **20** (Fig. 8).[50] In HEPES-buffered solution (20 mM, $CH_3CN : H_2O$, 3 : 7, v/v, pH = 7.0), probe **20** and Cd^{2+} follows a 1 : 1 binding ratio, making the solution immediately change from yellow to colorless and the absorption maximum blue-shift from 387 nm to 370 nm, and the absorbance has
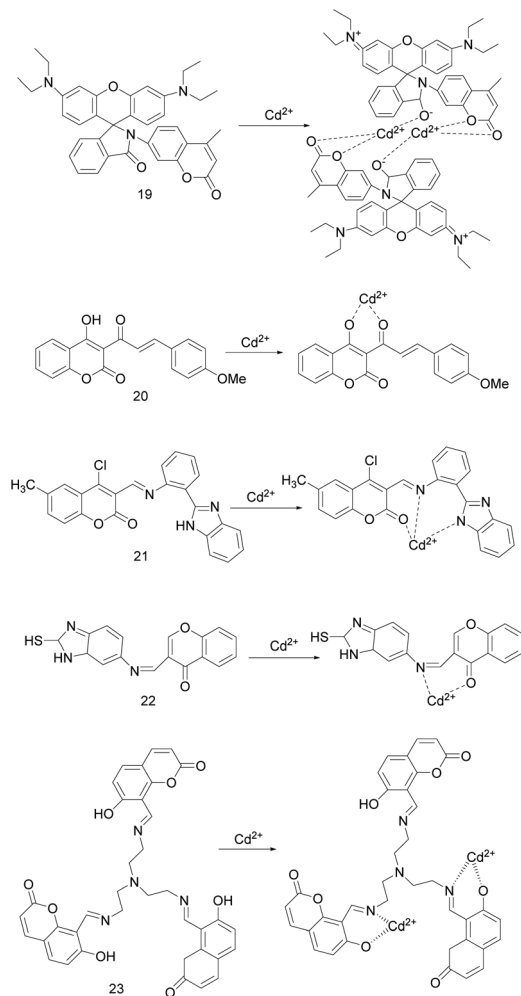
Fig. 8 Proposed binding mode of probes **19** to **23** with Cd^{2+}.

a good linear relationship with concentration of Cd^{2+}. When excited at 387 ± 3 nm, Cd^{2+} made the almost non-fluorescent probe **20** emit light blue fluorescence at 495 nm, and the fluorescence lifetime increase from 0.217 ns to 1.97 ns. According to Benesi–Hildebrand plot and nonlinear least squar fitting, the association constant for Cd^{2+} towards probe **20** were 9.56×10^5 M^{-1} and $(1.34 \pm 0.87) \times 10^6$ M^{-1}, respectively. Probe **20** does not respond to metal ions except Cd^{2+}, it can be used as a Cd^{2+} colorimetric and turn-on fluorescence probe. In mixed aqueous-organic media with the pH range of 7.0–9.0, it can detect Cd^{2+} as low as 5.84×10^{-8} M. Moreover, the test strip containing probe **20** can sense Cd^{2+}.

In 2018, K. Krishnaveni *et al.* reported a ratiometric probe **21** (Fig. 8) that based on ICT mechanism to recognize Cd^{2+}/F^-.[3] In CH_3CN/H_2O (1 : 9, v/v) buffered with HEPES (pH = 7.52), the probe **21** is combined with Cd^{2+}/F^- at a ratio of 1 : 1. Upon the excitation wavelength at 340 ± 5 nm, the fluorescence of probe **21** was changed by Cd^{2+} from pale yellow to dark yellow, and the fluorescence intensity ratio of $I_{418\,nm}/I_{530\,nm}$ was linearly related to the concentration of Cd^{2+}. The fluorescence of probe **21** can also be changed by F^-, and the fluorescence intensity ratio $I_{415\,nm}/I_{530\,nm}$ can quantitatively detect F^-. The binding constants of probe **21** for Cd^{2+} and F^- ions were 3.51×10^{-3} M

and 5.34×10^{-3} M, respectively. Probe **21** can be used as a high-selectivity and high-sensitivity proportional fluorescence sensor for Cd^{2+} and F^- with detection limits of 1.5×10^{-10} mol L^{-1} and 1.2×10^{-10} mol L^{-1}, respectively. In addition, probe **21** has reversibility (EDTA) and low cytotoxicity, and can be used for fluorescence imaging of Cd^{2+} in H9c2 cancer cells.

S. Zehra's team described coumarin derived turn-on probe **22** (Fig. 8) in 2019.[49] The spectral studies were carried out in a THF/H_2O (1 : 1) solution and an excitation at 300 ± 5 nm. Probe **22** chelating Cd^{2+} inhibited C=N isomerization of probe, so the fluorescence of probe **22** increased and the fluorescence emission intensity is linearly related to the Cd^{2+} of 1–15 μM. The probe **22** was combined with Cd^{2+} at 1 : 1 stoichiometry, the K_a was 3.3×10^5 M^{-1}, and the detection limit for Cd^{2+} was 0.114 μM. The response of probe **22** to Cd^{2+} is rapid and reversible (EDTA), without obvious interference from other metal ions, and can quantitatively detect the micro molar concentration of Cd^{2+} in the environmental and biological samples as well.

In 2019, Y. F. Tang's study group reported probe **23** (Fig. 8), in which coumarin is a fluorophore and tri-(2-aminoethyl)-amine is a selective recognition unit for Cd^{2+}.[34] In CH_3CN–HEPES (90 : 10, v/v, pH = 7.4) solution, the probe **23** binding to Cd^{2+} inhibited its C=N isomerization and PET process. When excited by 361 nm, probe **23** showed that the blue fluorescence was turned on, the fluorescence quantum yield increased, and the fluorescence emission peak shifted from 505 nm to 457 nm. Further, the fluorescence intensity was linearly related to the amount of Cd^{2+}. The probe **23** bound to Cd^{2+} in a 1 : 2 ratio, the association constants and detection limits were 1.37×10^{11} M^{-2} and 1.16×10^{-7} M, respectively. The probe **23** recognizes Cd^{2+} well and is only slightly interfered by Zn^{2+}. However, since EDTA makes probe **23** reversibly bind to Zn^{2+} and irreversibly bind to Cd^{2+}, the effect of Zn^{2+} can be eliminated. Therefore, it can be used as a high selectivity and sensitivity probe to detect Cd^{2+}. And it also can be as an imaging agent for fluorescence imaging of Cd^{2+} in HepG-2 cells.

The spectroscopic and analytical parameters of the coumarin-based Cd^{2+} fluorescent probes are compiled in Table 2. These probes recognizes Cd^{2+} according to different response mechanisms, and its value in practical application has been proved by test paper test, reversibility, pH application range and biological imaging. However, optimizing its water solubility, sensitivity, selectivity and anti-interference is still a problem to be solved in future research.

4. Benzothiazole based Cd^{2+} fluorescent sensor

Benzothiazole is an important type of heterocyclic ring containing N and S, which can be used as a fluorophore and is widely used in the design and construction of ion recognition probes.[21,24] In some cases, the N and S contained in it can also be used as a coordination site for ions.

In 2018, J. Li *et al.* described sensor **24** (Fig. 9).[4] The DMF/H_2O (9 : 1, v/v) solution and the excitation at 411 nm were selected as the exploration conditions. Due to the combined

Table 2 Spectroscopic and analytical parameters of the coumarin-based Cd^{2+} fluorescent probes

Probe	Solvent	Excitation wavelength (nm)	Emission wavelength (nm) λ_{em_0}–λ_{em}	Detection limit (nM)	Association constant	Interfering ion(s)	Ref.
19	CH_3OH–H_2O (2 : 1)	340	430–589	10.1	7.8×10^5 M^{-3}	—	2
20	CH_3CN–H_2O (3 : 7)	387	495	58.4	$(1.34 \pm 0.87) \times 10^6$ M^{-1}	—	50
21	CH_3CN–H_2O (1 : 9)	340	418	0.15	3.51×10^{-3} M	F^-	3
22	THF–H_2O (1 : 1)	300	About 360	114	3.3×10^5 M^{-1}	—	49
23	CH_3CN–H_2O (9 : 1)	361	505–457	116	1.37×10^{11} M^{-2}	Zn^{2+}	34

action of the ESIPT effect from the 2-(2-hydroxyphenyl)-benzothiazole moiety and AIE effect, sensor **24** exhibited weak orange fluorescence at 573 nm. The combination of sensor **24** with Zn^{2+} or Cd^{2+} inhibits the ESIPT effect and the PET process, thereby increasing the fluorescence emission, changing color from orange to yellow, and blue-shifting the fluorescence emission peak from 573 nm to 520 nm or 540 nm, respectively. The fluorescence intensity of the sensor **24** combined with Zn^{2+} or Cd^{2+} has a linear relationship with the concentration of Zn^{2+} or Cd^{2+}. The detection limits of sensor **24** for Zn^{2+} and Cd^{2+} are 0.036 μM, 1.16 μM, respectively. The binding constants are 3.27×10^4 M^{-1} and 2.93×10^3 M^{-1}, respectively. The addition of cysteine makes the complex of sensor **24** and Cd^{2+} restore the fluorescence signal of sensor **24**, while the complex of sensor **24** and Zn^{2+} only reduces the fluorescence intensity. Thus, cysteine can be used as an auxiliary agent in the probe detection of Zn^{2+} and Cd^{2+} to distinguish them. Moreover, sensor **24** can be used for optical cell imaging of Zn^{2+} or Cd^{2+} and on-site analysis of test paper.

The same year, R. Diana's research group designed probe **25** (Fig. 9) based on the ICT mechanism to respond to Cd^{2+}.[24] In ethanol–water solution, the probe **25** can quantitatively detect Fe^{3+} and Fe^{2+} through naked eye. Adding Zn^{2+}/Cd^{2+}, the fluorescence intensity of probe **25** increased by 3.25/4.35 times and the emission peak red-shifted from 348 nm to 370/375 nm. The

detection limits for Zn^{2+} and Cd^{2+} were 205 nM and 642 nM, respectively. The binding constant for Zn^{2+} and Cd^{2+} were log K_a = 4.10 and 4.25, respectively. To understand the mode of binding to the sensor, the complex of Zn^{2+} and the sensor is studied by X-ray crystallography, and the combination mode is shown in Fig. 10. However, due to the low selectivity, sensitivity, and anti-interference (such as: Fe^{3+}, Fe^{2+}, Co^{2+}), the probe **25** is difficult to meet the detection requirements.

In 2021, S. Paul et al. reported a multifunctional naphthalene-benzothiazole based sensor **26** (Fig. 9).[51] The donor part such as –C=N enhances the reliability of the sensor, and the active functional group such as –OH improves the color detection efficiency of the sensor for the target analyte. Sensor **26** (1×10^{-5} M, CH_3CN) can recognize Cd^{2+} in pure water by turning on fluorescence. When excited at 390 nm, due to the –C=N isomerization, PET, and ESIPT mechanism, the sensor exhibits weak green fluorescence emission at 505 nm. The combination of Cd^{2+} with sensor **26** increases the molecular rigidity, inhibits the effects of PET and ESIPT, and promotes the CHEF process, which leads to a significant increase in the fluorescence intensity of this sensor. The association constant (K_a) of the sensor with Cd^{2+} is 0.91×10^6 $M^{-1/2}$, and the
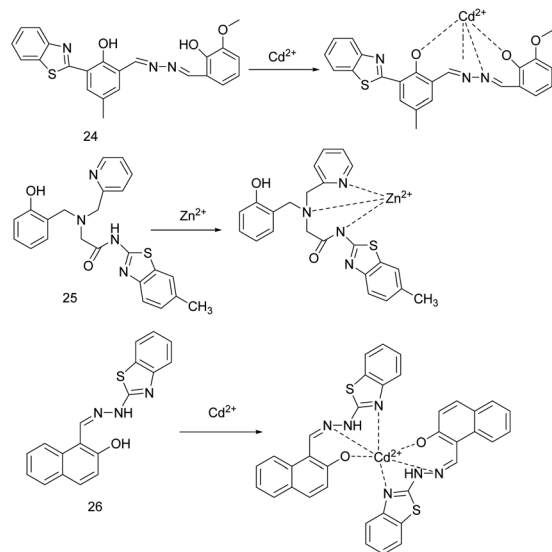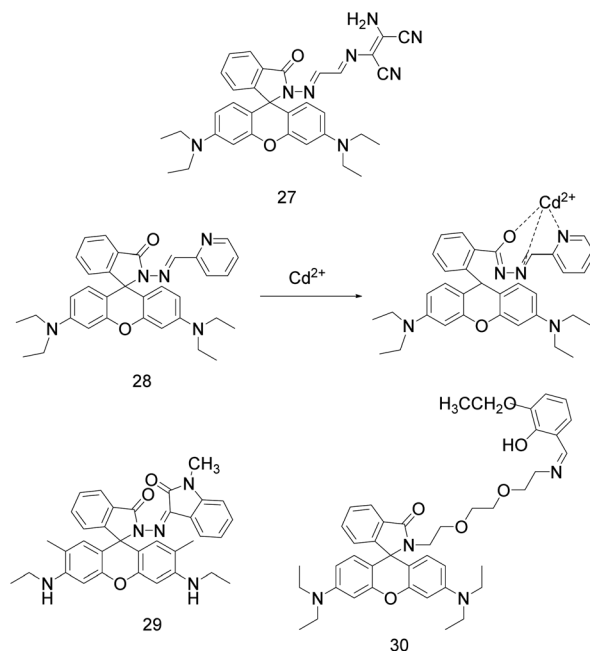

Fig. 9 Proposed binding mode of probes **24** to **26** with Cd^{2+}.

Fig. 10 The structure of probes **27** to **30**.

Table 3 Spectroscopic and analytical parameters of the benzothiazole-based Cd^{2+} fluorescent probes

Probe	Solvent	Excitation wavelength (nm)	Emission wavelength (nm) $\lambda_{em_0}-\lambda_{em}$	Detection limit (nM)	Association constant (K_a)	Interfering ion(s)	Ref.
24	DMF–H$_2$O (9 : 1)	411	573–540	1160	2.93×10^3 M^{-1}	Cysteine, Zn^{2+}	4
25	EtOH–H$_2$O	309	348–375	642	log K_a = 4.25	Fe^{3+}, Fe^{2+}, Co^{2+}, Zn^{2+}	24
26	CH$_3$CN	390	505	16.7	0.91×10^6 M$^{-1/2}$	Zn^{2+}, CN$^-$	51

detection limit for Cd^{2+} is 16.7 nM. This sensor can also detect Zn^{2+} or CN^- in pure water medium. In addition, sensor **26** has cell membrane permeability and biocompatibility, and can detect the content of Cd^{2+} and CN^- in bitter almonds and yeast cells.

Like quinoline and coumarin, benzothiazole can be used not only as fluorophore, but also as Cd^{2+} chelating site. We provide the spectroscopic and analytical parameters of these probes benzothiazole-based fluorophore in Table 3. These probes are responsive to multiple analytes and are also disturbed by a variety of ions. Among them, the probe **24** can recognize Zn^{2+} and Cd^{2+} at the same time. The research team uses cysteine as an auxiliary agent to distinguish Zn^{2+} and Cd^{2+}, which is also a way to eliminate interference and roughly identify Cd^{2+} in the environment. However, the quantitative detection of Cd^{2+} still needs a probe with high selectivity and anti-interference.

5. Rhodamine-based Cd^{2+} fluorescent sensor

Rhodamine derivatives possess high fluorescence quantum yield, photostability, large molar extinction coefficient, bioavailability, and its excitation wavelengths and emission wavelengths in the visible light region.[23,31] Furthermore, it exist an equilibrium between the nonfluorescent "spirolactam ring" and fluorescent "ring-open" forms to allow analyte sensing through "off–on" switching.[23,31,52] Therefore, it is widely used in the design of fluorescent sensors.

In 2017, P. Sakthivel's research group synthesized a rhodamine based senor **27** (Fig. 10) by linking to diaminomaleonitrile moiety.[52] This sensor can not only identify Cd^{2+} by naked eyes, but also can detect Cd^{2+} quantitatively by UV-vis absorption and fluorescence spectra. Upon addition of Cd^{2+}, an absorption peak emerged at 530 nm and the intensity had a linear relationship with Cd^{2+} concentration. Upon complexation, colourless spirolactam form is converted into colored ring opened amide form, which displays a noticeable naked-eye detection of the magenta. In HEPES buffer (acetonitrile–water = 7 : 3, 10 μM, pH = 7.54), sensor **27** was combined with Cd^{2+} in a ratio of 1 : 1, which increased its weak fluorescence emission at 553 nm by 200 times (excitation at 530 nm). When the Cd^{2+} concentration was 1.0×10^{-7} to 1.0×10^{-5} mol L^{-1}, the fluorescence intensity [$1/(F - F_0)$] at 553 nm had a linear relationship with $1/$[Cd^{2+}]. The association constant between sensor **27** and Cd^{2+} was 2.33×10^5 M^{-1}, and the detection limit of sensor **27** for Cd^{2+} was 18.5 nM. It can be used for the determination of Cd^{2+} in river and tap water samples and as an imaging agent for Cd^{2+} in living cells.

M. Maniyazagan *et al.* designed a rhodamine pyridine conjugated probe **28** (Fig. 10) based on FRET mechanism, which can recognize Cd^{2+} by colorimetry and fluorescence.[32] In ACN/ HEPES buffer (2 : 8, V/V, pH = 7.2, 10 mM), the probe was excited at 308 nm. With the addition of Cd^{2+}, probe **28** showed orange yellow fluorescence, the maximum emission wavelength red-shifted from 480 nm to 590 nm, and the solution changed from colorless to magenta. The recognition of Cd^{2+} by this probe is reversible (S^{2-}) and not interfered by other metal ions. In addition, probe **28** can also be used for imaging in HeLa cells at physiological pH. The binding constant of probe **28** to Cd^{2+} is 4.2524×10^4 M^{-1}, and the detection limit is 1.025×10^{-8} M. Probe **28** should be used in the pH range of 3–9, because the fluorescence induced by Cd^{2+} is stronger in high acidic environment, but it cannot be induced in alkaline environment due to the formation of $Cd(OH)_2$.

In the same year, W. Su *et al.* designed probe **29** (Fig. 10) by linking rhodamine 6G hydrazide with *N*-methylisatin *via* an imine linkage.[8] In EtOH/H$_2$O solution (9/1, 10 mmol HEPES buffer, pH = 7.2), probe **29** alone is non-fluorescent when excited at 500 nm. Upon the addition of Pb^{2+}, Hg^{2+}, Cd^{2+}, the probe **29** generated a yellowish-green fluorescence response to Cd^{2+}, while an orange fluorescence responses to Pb^{2+} and Hg^{2+}. And the fluorescence intensity at 560/560/552 nm had a linear relationship with the concentration of $Pb^{2+}/Hg^{2+}/Cd^{2+}$. The detection limits of probe **29** for Pb^{2+}, Hg^{2+} and Cd^{2+} were 1.6×10^{-8}, 1.2×10^{-8} and 4.7×10^{-8} mol L^{-1}, respectively. When EDTA was added to these complexes, the fluorescence response induced by Hg^{2+} and Cd^{2+} was reversible, while the fluorescence response induced by Pb^{2+} was irreversible. Therefore, probe **29** can be used as a multifunctional probe for detecting Pb^{2+}, Hg^{2+} and Cd^{2+}. Because the coexistence of Cd^{2+} with Pb^{2+} or Hg^{2+} can enhance the fluorescence of Cd^{2+}-induced, and the coexistence of Cd^{2+} with Cu^{2+} or Ni^{2+} can partially quench the fluorescence intensity of Cd^{2+}-induced, the selectivity and practicability of the probes **29** for Cd^{2+} are not enough.

In 2018, M. Ghosh and colleagues reported the probe **30** (Fig. 10) for trace-level detection and discrimination of Al^{3+}, Zn^{2+}, Cd^{2+}, Hg^{2+} in a ratiometric sensing mechanism involving PET–CHEF–FRET processes.[23] In 20 mM HEPES-buffered MeOH/H$_2$O (4/1, v/v, pH = 7.4) solution, probe **30** interacts with Cd^{2+} through phenolic hydroxyl group and "N" in C=N, "O" in alkane proton field to form 1 : 1 complex with Cd^{2+} at a low Cd^{2+} concentration and 1 : 2 at a high Cd^{2+} concentration. When excited at 306 nm, the fluorescence emission peak of probe **30** blue-shifted from 397 nm to 395 nm, the fluorescence intensity increased by 36 times, and the detection limit of probe **30** for Cd^{2+} was 6.7×10^{-9} M. The association constant of the
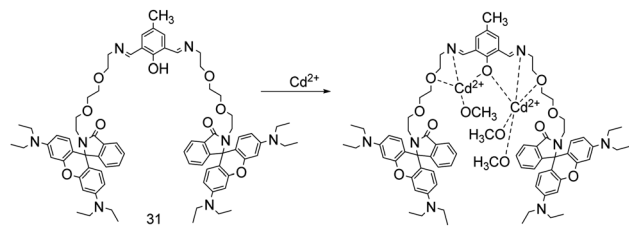
Fig. 11 Proposed binding mode of probe **31** with Cd^{2+}.

probe for Cd^{2+} is 1.35×10^5 M^{-1}, and its affinity for Cd^{2+} is higher than that for Zn^{2+}. It allows easy replacement of Zn^{2+} from the **30**-Zn adduct to form a more stable **30**-Cd adduct. Further, the simultaneous presence of Al^{3+} and Hg^{2+} can use KI to mask Hg^{2+}, while KI does not interfere with the emission profile of probe **30**. Probe **30** can identify low concentrations of Al^{3+} (pink), Zn^{2+} (green), Cd^{2+} (sky blue), Hg^{2+} (intense bloodred) according to different fluorescent signals without interference from other common ions, and can be used for imaging Zn^{2+}, Cd^{2+}, Hg^{2+} in squamous epithelial cells under a fluorescence microscope.

In 2019, a multi-signaling optical probe **31** (Fig. 11) reported by M. Banerjee's research group for rapid detection and discrimination of Zn^{2+}, Cd^{2+} and Hg^{2+} at nano-molar level.[31] In presence of Zn^{2+}, Cd^{2+} and Hg^{2+}, it emits deep red for Hg^{2+}, green for Zn^{2+} and blue for Cd^{2+} upon UV light irradiation. Interestingly, Hg^{2+} shows intense pink in bare eye. In HEPES-buffered aqueous methanol ($MeOH/H_2O$, 4/1, v/v, pH = 7.4), the combination of probe **31** and Cd^{2+} in a stoichiometric ratio of 1 : 2 makes the fluorescence emission (the excitation wavelength at 366 nm) peak blue-shift from 440 nm to 437 nm, and the blue fluorescence emission intensity is increased by 31 times. The binding constant of probe **31** for Cd^{2+} is 6.5×10^5 M^{-1}, and the detection limit is 9.6×10^{-9} M. Probe **31** can be used to detect Hg^{2+}, Cd^{2+}, Zn^{2+} at the nanomolar level, although the binding ability is sequentially weakened, KI can be used to mask Hg^{2+} interference, Na_2S can be used to mask Cd^{2+} interference.

The spectroscopic and analytical parameters rhodamine-based sensors are summarized in Table 4. Probes **27**, **28** and **29** have large emission wavelengths because their molecular structures have a large degree of conjugation, which makes the fluorescence emission peak appear at a large wavelength. Based on this mechanism, we can develop sensors with larger emission wavelength for environmental detection and biological imaging. In recent five years, rhodamine-based Cd^{2+} fluorescent

probes have good sensitivity, but their application is still disturbed by some ions. On the one hand, the probe responds to other analytes, on the other hand, the complex between the probe and Cd^{2+} is disturbed by other analytes. In the future development, it is necessary to optimize the ligands that recognize Cd^{2+}, so that the probe and Cd^{2+} have specific recognition ability and stable binding ability. At the same time, improving the water solubility and practicability of rhodamine-based probes is still the focus of future research.

6. Dansyl based Cd^{2+} fluorescent sensor

Dansyl group is fluorescent group with excellent performance as an electron acceptor, so it is used in the design of fluorescence sensors.[53] Biological studies have shown that metallothionein is a short peptide rich in cysteine, which has high affinity for a variety of heavy metals. Cd^{2+} and Cu^{2+} ions are the main metal binding with metallothionein.[54] Therefore, in the design of these probes' structure, P. Wang and co-workers introduced cysteine as the recognition group of Cd^{2+}, connected the recognition group and dansyl fluorophore through different spacer groups, and synthesized a series of highly selective probes **32–36** (Fig. 12) for Cd^{2+} by solid-phase peptide synthesis (SPPS) technology.[53,55–57] They described these Cd^{2+} fluorescent turn-on probes. These probes can be used to monitor Cd^{2+} in the environment and in living (HK2,[53,56,57] HeLa,[53–55] LNCaP[57]) cells. In general, they have good water solubility, selectivity, biocompatibility, and reversibility (EDTA,[55] cysteine[53]), and can be used for Cd^{2+} detection or bioimaging within some specific environments (example: Cd^{2+} concentration and pH).

In HEPES buffer (10 mM, pH = 7.4), under 365 nm UV lamp, probe **32** emits weak yellow fluorescence due to electron transfer from sulfhydryl group in Cys to dansyl group.[55] Binding to Cd^{2+} causes the PET process of probe **32** to be blocked, to enhance fluorescence intensity and to change from yellow to green fluorescence. Upon excitation at 330 ± 10 nm, the fluorescence intensity, quantum yield and lifetime were increased (4 times, from 0.0857 to 0.1769, from 9.32 ns to 17.36 ns). Probe **32** has large stokes shift for detecting Cd^{2+}, the binding constant is 5.18×10^{10} M^{-2}, and the detection limit is 45 nM. Probe **32** remains stable in 2–10 pH solution and has the strongest fluorescence signal induced by Cd^{2+} in 7–12 pH solution. In addition, the probe **32** can realize the reversible detection for Cd^{2+} by EDTA.

The probe **33** was synthesized by imitating the binding site of protein, in which tryptophan (energy donor, $\lambda_{ex} = 290$ nm, λ_{em}

Table 4 Spectroscopic and analytical parameters of the rhodamine-based Cd^{2+} fluorescent probes

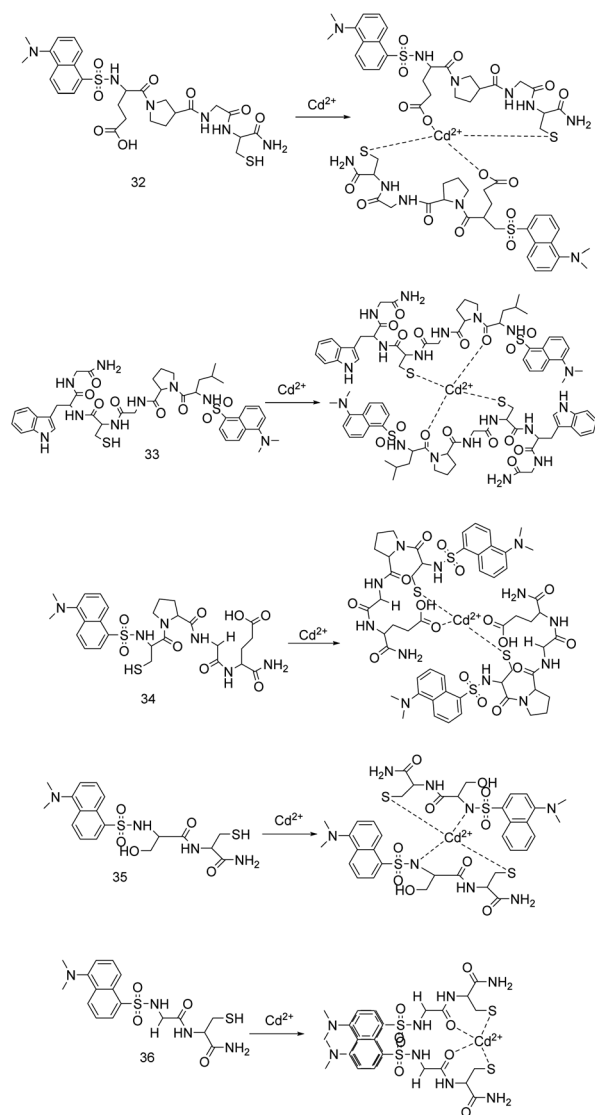| Probe	Solvent	Excitation wavelength (nm)	Emission wavelength (nm) $\lambda_{em_0}-\lambda_{em}$	Detection limit (nM)	Association constant (M^{-1})	Interfering ion(s)	Ref.
27	$CH_3CN–H_2O$ (7 : 3)	530	553	18.5	2.33×10^5	—	52
28	$CH_3CN–H_2O$ (2 : 8)	308	480–590	10.25	4.2524×10^4	S^{2-}	32
29	$EtOH–H_2O$ (9 : 1)	500	560	47	—	Pb^{2+}, Hg^{2+}, Cu^{2+}, Ni^{2+}	8
30	$MeOH–H_2O$ (4 : 1)	306	397–395	6.7	1.35×10^5	Al^{3+}, Hg^{2+}	23
31	$MeOH–H_2O$ (4 : 1)	366	440–437	9.6	6.5×10^5	Hg^{2+}, Zn^{2+}	31

Fig. 12 The probes structure reported by P. Wang's team and proposed binding mode with Cd^{2+}.

= 360 nm) and dansyl (energy acceptor, λ_{ex} = 330 nm, λ_{em} = 545 nm) are fluorophores and cysteine (recognition) is ionophore.[54] In the HEPES buffer (10 mM, pH = 7.4) solutions, the probe 33 can detect Cd^{2+} through two different excitation wavelengths. When excited at 290 ± 10 nm, probe 33 combines with Cd^{2+} to meet together the side chains of tryptophan and dansyl group to realize the FRET process, and the fluorescence emission increases

at 510 nm and decreases at 360 nm. When excited at 330 nm, the probe 33 binds to Cd^{2+} to increase the fluorescence emission intensity at 545 nm by 5 times (CHEF) and the lifetime from 8.32 ns and 16.33 ns. Under the 365 nm ultraviolet lamp, the solution of the probe 33 is added with Cd^{2+} to emit strong green fluorescence, and other metal ions are added to emit light brown weak fluorescence. The probe 33 is combined with Cd^{2+} at a stoichiometric ratio of 2 : 1, the binding constant is 9.12×10^{10} M^{-2}, and the detection limit is less than 27.5 nM. Further, the emission intensity of the complex remains almost unchanged at pH 7–9.

The dansyl-tetrapeptide fluorescent sensor 34 can produce a continuous "off–on–off" fluorescence response to Cd^{2+} and cysteine.[53] In the HEPES buffer solution (10.0 mM, pH = 7.4), upon excitation at 330 ± 10 nm, the sensor 34 through oxygen atoms of Glu and sulfhydryl of Cys binds to Cd^{2+} at 2 : 1, and the fluorescence changes from yellow to green. The fluorescence emission peak blue-shifts by 30 nm, and the fluorescence intensity increases. Adding Cys to the complex of sensor 34 and Cd^{2+} can restore the fluorescence signal of sensor 34. The detection limits for Cd^{2+} is 93 nM or for Cys is 35 nM, and lower than EPA or WHO guidelines.

Sensor 35 based on the conjugated dansyl group and dipeptide.[56] In HEPES buffer solutions (20.0 mM, pH = 7.4), under 365 nm ultraviolet light, the combination of sensor 35 and Cd^{2+} prevents the electron transfer from sulfhydryl group in Cys to the dansyl group (PET). Accordingly, the sensor 35 turns on green fluorescence. When excited at 330 nm, the fluorescence intensity at 545 nm is linearly related to the Cd^{2+} of 0–1.40 μM. The association constant and detection limit for Cd^{2+} are 1.30×10^9 M^{-2} and 13.8 nM, respectively. Sensor 35 can be used to detect Cd^{2+} with a pH range of 7.0–10.0. Due to the paramagnetism of Cu^{2+}, fluorescence of the complex of sensor 35 and Cd^{2+} is partially weakened, but there is no interference from other metal ions.

In 2019, they described probe 36 based on dansyl-appended dipeptide (Gly–Cys–NH_2).[57] In 20.0 mM HEPES buffer solution at pH 7.4, the addition of Cd^{2+} led to the fluorescence enhancement of the probe, and the formation of dansulfonyl dimer shifted the fluorescence emission peak from 560 nm to 515 nm (monomer-excimer mechanism). The addition of Cu^{2+} led to the fluorescence quenching of the probe. Under 365 nm UV light, the fluorescence of probe 36 was bright green and the emission was significantly enhanced with the addition of Cd^{2+}, while the fluorescence of the probe was dark brown and the emission was significantly quenched with the addition of Cu^{2+}. The binding constants of probe 36 to Cd^{2+} and Cu^{2+} are 1.74 ×

Table 5 Spectroscopic and analytical parameters of the dansyl-based Cd^{2+} fluorescent probes

Probe	Solvent	Excitation wavelength (nm)	Emission wavelength (nm) λ_{em_0}–λ_{em}	Detection limit (nM)	Association constant	Interfering ion(s)	Ref.
32	H_2O	330	550	45	5.18×10^{10} M^{-2}	—	55
33	H_2O	330	545	27.5	9.12×10^{10} M^{-2}	—	54
34	H_2O	330	About 570–540	93	—	—	53
35	H_2O	330	545	13.8	1.30×10^9 M^{-2}	Cu^{2+}	56
36	H_2O	365	560–515	14.5	1.74×10^8 M^{-2}	Cu^{2+}	57

10^8 M^{-2} and 6.96×10^7 M^{-2}, respectively. The detection limits for Cd^{2+} and Cu^{2+} are 14.5 nM and 26.3 nM, respectively. The probe with pH 7–12 can stably recognize Cd^{2+} (pH 7.0–12.0) and Cu^{2+} (pH 2.0–12.0) in 20 s, and is not interfered by other metal ions and anions. In addition, probe **36** has hypotoxicity, membrane permeability and low toxicity, which can be used to detect Cd^{2+} and Cu^{2+} in living LNCaP cells.

The spectroscopic and analytical parameters danyl-based fluorescent probes are shown in Table 5. The researchers took the sulfhydryl group in cysteine as the recognition site of Cd^{2+}, and designed and synthesized these probes by changing the type, number and position of linkers, so as to improve the sensitivity, selectivity and anti-interference of theses probes. Moreover, the researchers use amino acids as recognition groups and linkers, which has low toxicity for biological monitoring. These sensors have good water solubility, selectivity, sensitivity and long emission wavelength. They can be used not only for environmental monitoring, but also for cell imaging.

7. Diarylethylene based Cd^{2+} fluorescent sensor

Diarylethylene is composed of heteroaromatic ring groups connected on both sides of the vinyl group. The distance between the two aryl groups is relatively close, which can form two isomers of ring opening and ring closure. As a good photochromic dye, diarylethylene has the advantages of excellent photochromic performance, thermal stability, fatigue resistance, feasible synthesis, high photoisomerization quantum yields, and convenient functionalization.[21,22,28] Therefore, it is often used as a fluorophore part in the design of probes. Diarylethene fluorescent probes have two states: ring-open and ring-closed, which can be converted under ultraviolet light (from ring-open to ring-closed) and visible light. Since the ring-open and ring-closed positions of all diarylethene probes are the same, and the state of the ring does not affect the binding site with Cd^{2+}. Therefore, the probe **37** is taken as an example to show the ring-open and ring-closed state of diarylethylene.

In 2017, D. B. Zhang's research group synthesized probe **37** (Fig. 13), which can switch between ring-open and ring-closed under the light irradiation at 297 nm and >500 nm.[21] In acetonitrile solution, the addition of Cd^{2+}/Zn^{2+} changed the probe **37** solution from colourless to light-yellow/dark-yellow. Upon excitation at 402 nm, the fluorescence emission red-shifted from 519 nm to 559 nm/608 nm, and the fluorescence changed from dark to bright-yellow/orange. Under 297 nm light irradiation, the ring-open complex of Cd^{2+} and probe **37** changed into a ring-closed complex, and the fluorescence intensity of the complex was quenched by 8.7%/19%. The fluorescence of the ring-open complex was recovered under the irradiation light >500 nm. The detection limits of probe **37** for Cd^{2+} is 3.2×10^{-7} M and for Zn^{2+} is 2.88×10^{-7} M, and the association constants (log K_a) for Cd^{2+} is 3.81 and for Zn^{2+} is 3.51. Probe **37** is selective and reversible (EDTA) for the detection of Zn^{2+} and Cd^{2+}. The water solubility of the probe **37** is
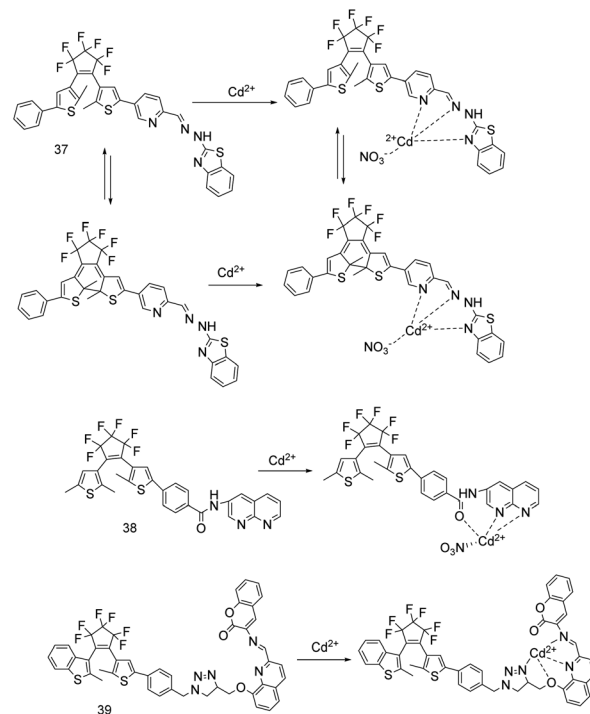

Fig. 13 Proposed binding mode of probes **37** to **39** with Cd^{2+}.

poor, and its coordination ability to Cd^{2+} is stronger than that to Zn^{2+}, so Cd^{2+} can replace Zn^{2+} binding probe **37**. A logic circuit was constructed with stimuli of UV/vis lights, Cd^{2+} and EDTA as inputs and fluorescence intensity at 559 nm as an output. In addition, because probe **37** contains a hydrazinobenzothiazole group, it can react with acids and bases, and the present of OH$^-$ is detected in the near infrared region.

In the same year, X. X. Zhang *et al.* reported that sensor **38** (Fig. 13).[22] In THF solution, under 360 nm light, adding Cd^{2+}, Ag$^+$, Zn^{2+} increases the fluorescence of sensor **38**, but only Cd^{2+} makes the fluorescence emission peak redshift from 439 nm to 541 nm and the fluorescence changes from dark to bright-green. 0–3.0 equiv. of Cd^{2+} has a linear relationship with the fluorescence intensity ratio ($I_{541\ nm}/I_{439\ nm}$). The ring-open and ring-closed states of sensor **38** can be converted by 313 nm and >450 nm light. Under 313 nm irradiation, the solution changes from pale yellow to magenta, and the fluorescence intensity reduces by about 87% compared with the open-ring complex. The sensor **38** detects Cd^{2+} with selectivity and reversibility, the detection limit for Cd^{2+} is 1.97×10^{-7} mol L^{-1}, and the binding constant (K_a) to Cd^{2+} is 8.60×10^3 L mol^{-1}. A logic circuit was fabricated with four inputs of the combinational stimuli of UV/vis and Cd^{2+}/EDTA, and one output of fluorescence intensity at 541 nm.

In 2018, S. Guo and colleagues designed probe **39** (Fig. 13) and studied its recognition of Cd^{2+} in 392 nm excitation and acetonitrile solution.[58] When Cd^{2+} was added, the solution of the open-ring isomer of probe **39** changed from colorless to yellow, the fluorescence emission peak red-shifted from 507 nm to 633 nm, the fluorescence changed from dark cyan to golden yellow, and the fluorescence intensity increased by 24.9 fold.

After illuminating at 297 nm, a complex of the closed-ring isomer of probe **39** and Cd^{2+} was formed, the solution changed from yellow to plum and appeared absorption band at 547 nm, the fluorescence changed from golden yellow to fawn brown. Cd^{2+} was directly added to probe **39** solution of closed-ring isomer, the color changed from purple to plum, and the fluorescence changed from dark to fawn brown. Due to the incomplete cyclization and the formation of parallel conformational isomers, the compound fluorescence of the ring-closed and Cd^{2+} was reduced by 34%. In addition, HSO_3^- made the probe **39** emit bright cyan fluorescence and increase the intensity 135 times. The probe **39** can recognize Cd^{2+} and HSO_3^- with high selectivity in the acetonitrile solution, and the binding with Cd^{2+} is irreversible.

In 2018, Z. Wang *et al.* synthesized the sensors **40** and **41** (Fig. 14), the conversion between their open-ring and closed-ring isomers can be realized by irradiation at 297 nm and >500 nm.[18,28] The properties of the two probes were studied in methanol solution and 350 nm light excitation. Because EDTA can make these probes bind to Cd^{2+} reversibly, the author used Cd^{2+}/EDTA and UV/vis as the input stimulus and the fluorescence intensity (sensors **40** and **41** were recorded at 476 nm and 480 nm, respectively) of probes in the presence of Cd^{2+} as the output to construct the logic circuit.

Sensor **40** has a dark purple weak fluorescence at 435 nm.[28] Adding Cd^{2+}, the C=N isomerization of the sensor was inhibited, the fluorescence changed from blue to bright blue, and maximum emission peak red-shifted from 435 nm to 476 nm. Under 297 nm, the colorless open-ring isomer transforms into pink closed-ring isomer, the emission intensity at 435 nm reduces about 73% and the fluorescence changes from blue to dark, and adding Cd^{2+} makes the fluorescence change from dark to dark blue. Sensor **40** can detect Cd^{2+} as low as 2.52×10^{-7} mol L^{-1}, and the binding constant (K_a) is 4.3×10^3 mol^{-1}. Sensor **40** with poor water solubility, and the fluorescence of Cd^{2+}-induced can be completely quenched by Cu^{2+}.

Sensor **41** chelates Cd^{2+}/Zn^{2+}, which inhibits the C=N isomerization, increases (51.1/17.7 fold) the fluorescence, and changes from dark to light-blue/green fluorescence.[18] In addition, the emission peak at 451 nm red shifts to 480 nm/500 nm, and the fluorescence intensity at 480 nm/500 nm is linearly related to the concentration of Cd^{2+}/Zn^{2+}. The complexing constants of open-ring isomer for Cd^{2+} is 5.95×10^4 L mol^{-1} and for Zn^{2+} is 4.9×10^4 L mol^{-1}, and the detection limits for Cd^{2+} is 8.69×10^{-9} mol L^{-1} and for Zn^{2+} is 3.67×10^{-8} mol L^{-1}. Under the irradiation at 297 nm, the open-ring isomer became a weaker fluorescent closed-ring isomer and the solution change from colorless to purple. Adding Cd^{2+}/Zn^{2+} made it change from light dark fluorescence to dark-blue/dark-green, the fluorescence intensity increase by 28.5/14.5 times, and the emission peak red-shift 29 nm/49 nm. Probe **41** can selectively and reversibly distinguish Cd^{2+} and Zn^{2+}.

In 2019, H. L. Liu *et al.* designed a fluorescence enhanced probe **42** (Fig. 15) based on C=N isomerism suppression and CHEF mechanism to identify Cd^{2+}.[25] They tested the probe in methanol solution and at 350 nm excitation wavelength. The open-ring isomer of probe **42** combined with Cd^{2+} increased the fluorescence emission intensity by 106 times, red-shifted the emission peak from 452 nm to 506 nm, and changed the fluorescence from dark to cyan. The association constant between probe and Cd^{2+} was 3.14×10^4 L mol^{-1}, and the detection limit for Cd^{2+} was 1.89×10^{-7} mol L^{-1}. The closed-ring isomer of probe **42** changed from non-fluorescent to dark-cyan fluorescence after binding to Cd^{2+}, and the emission peak red-shifted from 452 nm to 511 nm. Due to the formation of the closed-ring isomer and the FRET process from 2-aminoisoindole-1,3-dione to diethylene unit, its fluorescence intensity is 63% weaker than that of the complex of Cd^{2+} and the open-ring isomer. With 297 nm and >500 nm light irradiations, the conversion between the open-ring isomer and the closed-ring isomer of probe **42** can be realized. Adding Cu^{2+} made the open-ring isomer solution of probe **42** changed from colorless to yellow and the closed-ring isomer solution from purple to green, and it can be used for naked eye colorimetric detection of Cu^{2+} with the detection limit 4.12×10^{-8} mol L^{-1}. As a multifunctional fluorescent probe, the probe **42** can selectively and reversibly bind and accurately detect Cd^{2+} and Cu^{2+}, but Cu^{2+} can obviously quench the fluorescence intensity caused by Cd^{2+}.

J. F. Lv's research group designed and synthesized a multifunctional fluorescent sensor **43** (Fig. 15) based on diarylethene containing pyrene unit.[59] In acetonitrile solution, adding Cd^{2+}

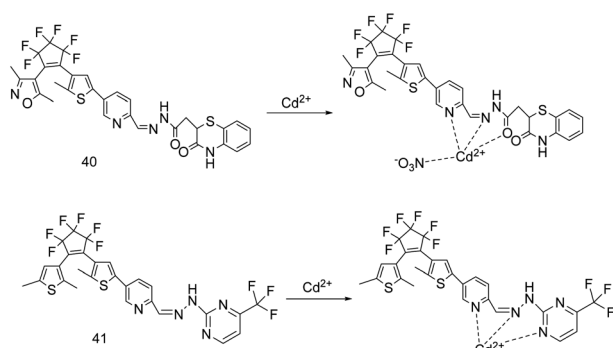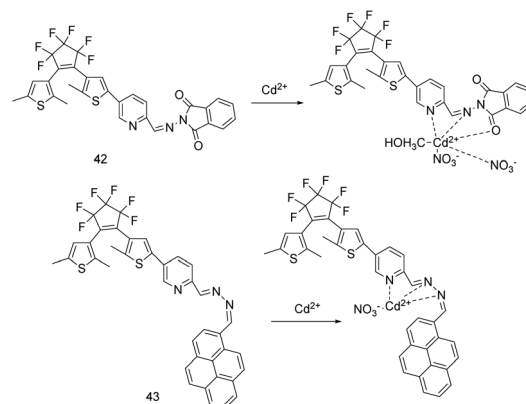**Fig. 14** The probes structure reported by Z. Wang's team and proposed binding mode with Cd^{2+}.

Fig. 15 Proposed binding mode of probes **42** and **43** with Cd^{2+}.

Table 6 Spectroscopic and analytical parameters of the diarylethylene-based Cd^{2+} fluorescent probes

Probe	Solvent	Excitation wavelength (nm)	Emission wavelength (nm) $\lambda_{em_0}-\lambda_{em}$	Detection limit (nM)	Association constant (K_a)	Interfering ion(s)	Ref.
37	CH$_3$CN	402	519–559	320	log K_a = 3.81	Zn^{2+}	13
38	THF	360	439–541	197	8.60×10^3 M^{-1}	Ag$^+$, Cu^{2+}, Pb^{2+}	22
39	CH$_3$CN	392	507–633	—	—	Cu^{2+}	58
40	MeOH	350	435–476	252	4.3×10^3 M^{-1}	Cu^{2+}	28
41	MeOH	350	451–480	8.69	5.95×10^4 M^{-1}	Zn^{2+}	18
42	MeOH	350	452–506	189	3.14×10^4 M^{-1}	Cu^{2+}	25
43	CH$_3$CN	440	648	1.85	5.8×10^4 M^{-1}	Mg^{2+}, Zn^{2+}, Sn^{2+}, Co^{2+}, Cu^{2+}, Ni^{2+}	59

or Zn^{2+} makes the absorption peak of the sensor red shift and the solution color change. Under the excitation at 440 nm, the presence of Cd^{2+} or Zn^{2+} not only changes the fluorescence color, but also increases the fluorescence intensity (due to the C=N isomerization blocking and CHEF effect), and the fluorescence emission intensity is linearly related to a certain range of ion concentration. The binding constants of the open-loop sensor with Cd^{2+} or Zn^{2+} are 5.8×10^4 L mol^{-1} or 6.0×10^4 L mol^{-1}, respectively. The detection limits for Cd^{2+} or Zn^{2+} are 1.85×10^{-9} mol L^{-1} or 7.68×10^{-9} mol L^{-1}, respectively. Sensor **43** can be used for the detection of Cd^{2+} and Zn^{2+} in actual water samples, and processed into test pieces for on-site analysis and testing. However, when the sensor is used for the fluorescence detection of Cd^{2+} (affected by Mg^{2+}, Zn^{2+}, Sn^{2+}, Co^{2+}, Cu^{2+}, Ni^{2+}) and Zn^{2+} (affected by Cd^{2+}, Hg^{2+}, Cu^{2+}, Ni^{2+}), it is easy to be interfered by a variety of cations. Moreover, because the absorption peak, emission peak and color change caused by Cd^{2+} or Zn^{2+} are relatively close, sensor **43** can't distinguish them effectively by naked eye.

The spectroscopic and analytical parameters of the diarylethene-based Cd^{2+} fluorescence sensor are shown in Table 6. Different from fluorophores such as quinoline, coumarin and benzothiazole, diarylethylene is only used as fluorophore (signal reporter) in probe design. The diarylethylene-based probes can realize the ring-open and ring-closed transition through ultraviolet and visible light, and its ring-open state recognition Cd^{2+} can produce greater fluorescence changes. Some sensors diarylethylene-based have relatively large emission wavelengths. However, many sensors either respond to ions other than Cd^{2+}, or are disturbed by other ions when detecting Cd^{2+}, and have low selectivity and anti-interference ability. Moreover, their water solubility and detection limit need to be improved.

8. Other small organic molecules based Cd^{2+} sensor

In 2017, S. Chithiraikumar's research group synthesized sensor **44** (Fig. 16), which can recognize Cd^{2+} through absorption and fluorescence spectra.[12] In acetonitrile/HEPES buffer medium (5 mM, pH = 7.3, 1 : 5, v/v), the sensor **44** combines with Cd^{2+} to red-shift its maximum absorption from 391 nm to 418 nm, and the absorbance of probe at 418 nm to increase with the concentration of Cd^{2+}, and the association constant for Cd^{2+}

was 5.39×10^5 M^{-1} ($\pm 1.0\%$). Under the excitation at 400 nm, the sensor **44** binds to Cd^{2+} with an association constant of 3.16×10^5 M^{-1}, which makes the fluorescence emission peak redshift from 558 nm to 561 nm, and the fluorescence emission intensity and quantum yield increase. The sensor **44** binds to Cd^{2+} in a pH system of 4.2 to 8.1, rapidly increases fluorescence within 0.3 min and without interference from various ions to monitor Cd^{2+} as low as 10.21 nM. The sensor **44** has selectivity, sensitivity, reversibility (EDTA) and bio-imaging (HeLa cells) for detecting Cd^{2+}, the fluorescence response is enhanced when the temperature increases within 25–45 °C, and the fluorescence is quenched when the aqueous buffer is 80–100%.

D. D. Cheng and colleagues reported on the ICT probe **45** (Fig. 16) with tetramethyl substituted bis(difluoroboron)-1,2-bis [(1H-pyrrol-2-yl)methylene]hydrazine (Me$_4$BOPHY) as a fluorophore and N,N-bis(pyridin-2-ylmethyl)benzenamine (BPA) as an electron donor moiety.[19] Chelating Cd^{2+} reduces the electron-donating ability of BPA, thus quenching ICT transition and initiating π–π transition of the fluorophore, resulting in blue
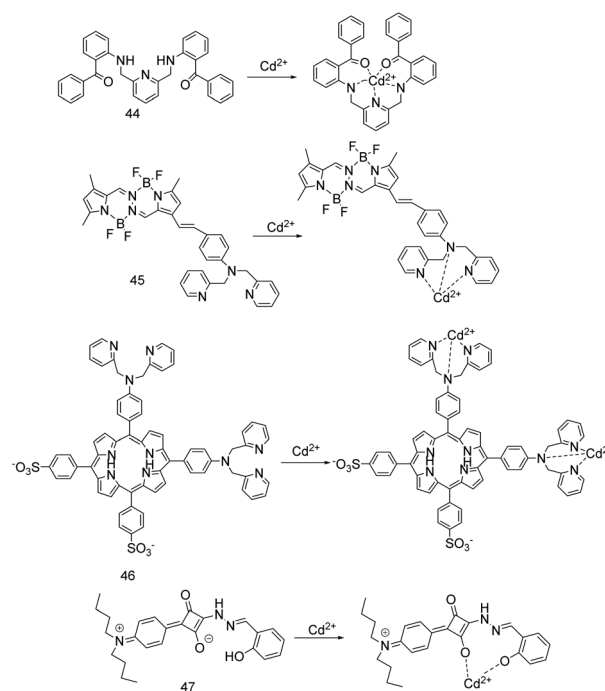
Fig. 16 Proposed binding mode of probes **44** to **47** with Cd^{2+}.

shift of the absorption and emission of the probe. In acetonitrile solution, Cd^{2+} made the absorption peak of probe **45** blue-shift from 550 nm to 475 nm. Under the excitation at 410 ± 10 nm, the fluorescence emission peak blue-shifted from 675 nm to 570 nm, and the solution changed from red to bright yellow. When the excitation wavelength at 495 nm, the fluorescence intensity ratio $F_{570\ nm}/F_{730\ nm}$ reached a stable value within 1 min and had a functional relationship with the concentration of Cd^{2+}, which could be used to quantitatively detect Cd^{2+}. The probe **45** also has a fluorescence response to Zn^{2+}, but still emits red fluorescence. Therefore, the probe **45** can detect Cd^{2+} as low as 6.9 nM or 0.77 ppb with selectivity, sensitivity, and anti-interference, which is far below the safety value (3 ppb) set for drinking water by WHO.

W. B. Huang *et al.* synthesized probe **46** (Fig. 16), in which DPA was used as the recognition group of Cd^{2+}, and two sulfonic groups were introduced into the porphyrin fluorophore to enhance the water solubility.[60] The HEPES buffer (20 mM, pH = 7.4) and the excitation at 418 nm were selected to study. Probe **46** and Cd^{2+} combined with a stoichiometric ratio of 1 : 2, weakened the conjugation between DPA and porphyrin (ICT), so that the fluorescence emission blue-shifted from 653 nm to 611 nm, and the fluorescence intensity ratio of $F_{611\ nm}/F_{653\ nm}$ was linearly related to the Cd^{2+} concentration of 0–2.5 μM. The dissociation constant was 31.2 ± 5.2 μM, and the detection limit for Cd^{2+} was 3.2×10^{-8} M. Hg^{2+} and Cu^{2+} showed moderately quenching of fluorescence signal at 653 nm, but there was no enhancement of fluorescence signal at 611 nm. In an environment with no Hg^{2+} or Cu^{2+} and a pH of 6.5–10, the probe **46** can quantitatively and reversibly (EDTA) detect Cd^{2+}. In addition, the probe has low cytotoxicity and can be used for bio-imaging in living cells.

J. Q. Sun's research group designed a multi-responsive squaraine-based sensor **47** (Fig. 16).[17] In ethanol/H_2O (9 : 1) solution (10 mM HEPES buffer at pH 7.0), when excited at 470 nm, sensor **47** shows weak fluorescence at 545 nm due to ESIPT and C=N isomerization. Adding $Cd^{2+}/Al^{3+}/Zn^{2+}$ made the sensor **47** increase the fluorescence intensity by 39/31/53 times, and shift the emission peak from 545 nm to 537 nm/550 nm/542 nm, and emit bright-green/yellow/yellow-green fluorescence under 365 nm irradiation. The stability of the combination of sensor **47** with Al^{3+}, Zn^{2+}, Cd^{2+} decreased in turn. Sensor **47** can detect Cd^{2+} as low as 5.76×10^{-8} M at pH 5–10, and all the other metal ions except Zn^{2+} can decrease the fluorescence enhancement caused by Cd^{2+} to a different extent. Moreover, the sensor **47** can chelate Al^{3+} from Aβ1-42-Al complex, indicating its potential value in the treatment of Alzheimer's disease.

N. A. Bumagina *et al.* described probe **48** (Fig. 17), which was excited at 495 nm and studied its ion recognition in a solution of propanol-1/cyclohexane (1 : 30).[61] Adding Cd^{2+}/Hg^{2+} made the fluorescence change from yellow-orange to orange-green, and the maximum emission peak of probe **48** red-shift from 518 nm to 538 nm/539 nm. When the molar ratio of Cd^{2+} concentration to probe concentration is less than 5, the fluorescence intensity increases linearly with the increase of Cd^{2+} concentration. When the molar ratio of Cd^{2+} concentration to probe concentration is greater than 5, the ratio of $I_{538\ nm}/I_{518\ nm}$
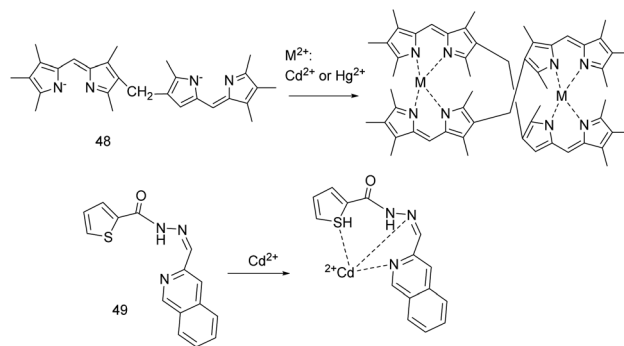

Fig. 17 Proposed binding mode of probes **48** and **49** with Cd^{2+}.

increases to 150 times and remains unchanged. Similarly, when the molar ratio of Hg^{2+} concentration to probe concentration is greater than 4, $I_{539\ nm}/I_{518\ nm}$ increases by 40 times and remains unchanged. Probe **48** complexes Cd^{2+}/Hg^{2+} with a stoichiometric ratio of 2 : 2, and the detection limit is 2×10^{-9} M/1.7×10^{-8} M, which can effectively detect Hg^{2+}, but Co^{2+}, Cu^{2+}, Zn^{2+}, Hg^{2+} interfere with the detection of Cd^{2+}.

The sensor **49** (Fig. 17) synthesized by V. Tekuri *et al.* has good selectivity, precision and accuracy for the detection of Cd^{2+}, and can be used for colorimetric detection of Cd^{2+} in environmental samples.[62] When Cd^{2+} was added to the DMF solution of the new heterocyclic thiophene-2-carboxylic acid hydrazide based sensor **49**, the solution changed from colorless to yellow, the maximum absorption red-shifted from 320 nm to 425 nm, and the absorption intensity had a linear relationship with the concentration of Cd^{2+} from 5.0 to 30 μM. The association constant (K_a) was 3.7×10^4 M^{-1}, and the detection limit was 2.0×10^{-7} M.

Y. Tang's research group synthesized probe **50** (Fig. 18) by a click reaction of dialkyne and indole azide precursors.[63] In ethanol–ethyl acetate (7 : 3, v/v) solution, under 283 nm, adding Cd^{2+}/Fe^{3+} made the maximum fluorescence emission of probe **50** at 510 nm be quenched. But only the concentration of Cd^{2+} from 0 to 7.226×10^{-5} M was linearly related to the fluorescence intensity, which can be used to quantitatively detect Cd^{2+},
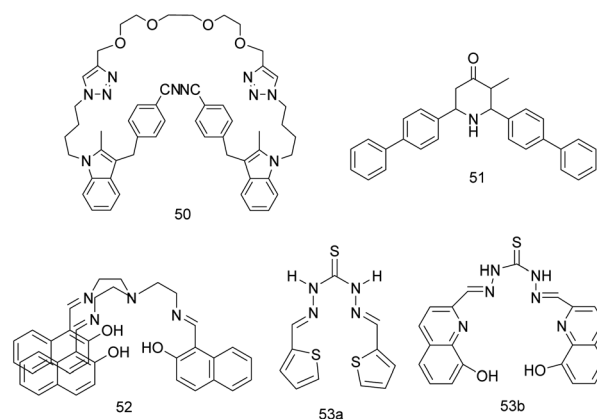

Fig. 18 The structure of probes **50** to **53**.

and the detect limit for Cd^{2+} is 2.69 μM. The fluorescence quenching of probe **50** by Cd^{2+} reached equilibrium within 30 minutes, and it was obviously quenched at 20–50 °C, and reached the best quenching at 70 °C.

The biphenyl substituted piperidine-4-one sensor **51** (Fig. 18) in aqueous solution containing 1% CH_3CN, upon irradiation at 315 nm, the fluorescence at 433 nm was increased by 3.6 times with the addition of Cd^{2+}.[64] And the maximum fluorescence intensity of sensor **51** has a linear relationship with the Cd^{2+} concentration of 0 to 110 equivalents, which can quantitatively detect Cd^{2+}. The binding constant and the detection limit for Cd^{2+} were 3862.872 M^{-1} and 1×10^{-7} mol L^{-1}, respectively. The sensor **51** reported by S. Poomalai *et al.* can selectively and sensitively respond to Cd^{2+} in the pH range of 4.5 to 8.0, and can be incorporated into the prepared polysulfone membranes to effectively detect and remove Cd^{2+} in real samples.[64]

The first report of probe **52** (Fig. 18) was reported by W. H. Hsieh *et al.* in 2012 as a probe for Zn^{2+} recognition.[65] In 2017, P. Kaur *et al.* supplemented the ion recognition of this probe.[66] In methanol solution, the solution immediately changed from yellow to colorless when probe **52** and Zn^{2+}/Cd^{2+} were combined at a ratio of 1 : 2. The probe **52** chelated Zn^{2+}/Cd^{2+} to inhibit C=N isomerization. Upon excitation at 308 nm, adding Zn^{2+} and Cd^{2+} made probe **52** turn on fluorescence at 450 nm, the detection limits for Zn^{2+} was 86 nM and for Cd^{2+} was 50 nM, and the binding constant with Zn^{2+} was 4.60 and for Cd^{2+} was 4.87. If there is IO_4^- in the detection system, there is no turn-on fluorescence response caused by Zn^{2+}/Cd^{2+}. In addition, the probe **52** can distinguish Fe^{3+} (light green) and Fe^{2+} (purple) by naked eye.

In 2017, the study team of B. K. Momidi designed the multi-signaling thiocarbohydrazide based colorimetric sensor **53a** and **53b** (Fig. 18).[67] **53a** can specifically bind to Cd^{2+}, **53b** can multi-signal response to Hg^{2+}, Cu^{2+}, Cd^{2+}, Pb^{2+} and the selectivity is sequentially weakened, and both sensors have good linear range $0–10^{-6}$ M, which can quantitatively detect metal ions in aqueous medium. In DMSO solution, **53a** has no response to other metal ions, but when combined with Cd^{2+} at a stoichiometric ratio of 1 : 1 in DMSO solution, the solution changes from colorless to pale pink, and the maximum absorption band red-shifts from 395 nm to 579 nm. The detection limit of **53a** for Cd^{2+} is 3.22 μM. In DMF solution, **53b** has an absorption band at 354 nm. When **53b** reacts with Cd^{2+}, Hg^{2+}, Cu^{2+} and Pb^{2+} at a stoichiometric ratio of 1 : 1, the solution changes from colorless to brownish-red, pink, yellow and orange, and the absorption peaks shows red shifted by 146 nm, 96 nm, 66 nm and 96 nm, respectively. The detection limits of **53b** for Cd^{2+}, Hg^{2+}, Cu^{2+} and Pb^{2+} are 0.20 μM, 0.70 μM, 0.20 μM and 0.30 μM, respectively. The multi-sensing ability of **53b** is due to the presence of hydroxy functionality of quinoline moiety, which has suitable binding sites (–OH, C=N and N in quinoline ring) to co-ordinate with the metal ions.

V. Kumar's team synthesized a sensor **54** (Fig. 19) with biphenyl as the fluorophore and carboxylic acid group as the binding site.[68] In CH_3OH solution, under excitation at 320 nm, sensor **54** emits strong fluorescence at 418 nm. Adding Cd^{2+} made the fluorescence emission peak blue-shift of sensor **54** by
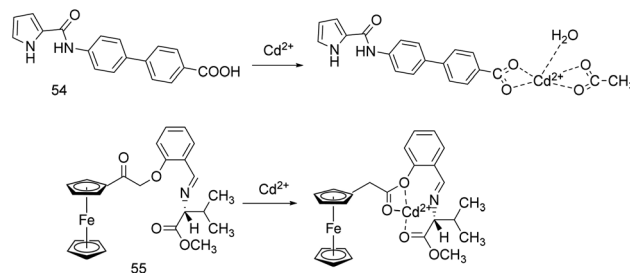

Fig. 19 Proposed binding mode of probes **54** and **55** with Cd^{2+}.

25 nm and the fluorescence be quenched. Adding Al^{3+} made the fluorescence emission peak of sensor **54** red-shift 3 nm and fluorescence be increased. Adding S^{2-} made the fluorescence emission peak of sensor **54** blue shift by 7 nm and the fluorescence be quenched. The sensor **54** combines Cd^{2+}, Al^{3+}, and S^{2-} at a stoichiometric ratio of 1 : 1, and the detection limits for them are 1.02 μM, 0.55 μM, and 16.57 μM, respectively. When Cd^{2+}, Al^{3+}, and S^{2-} exist at the same condition, the combination of sensor **54** and Al^{3+} is dominant, and K_2HPO_4 can realize the reversibility of sensor **54** to detect Cd^{2+}/Al^{3+}.

Among the probes reported in 2017, in addition to those mentioned above, there is a ferrocenyl Schiff base sensor **55** (Fig. 19) reported by M. Findik's team.[69] In an acetonitrile solution and an excitation at 378 nm, the sensor **55** bound to Zn^{2+}/Cd^{2+} enhanced the weak fluorescence emission at 452 nm by 12.73/4.59 times (due to the C=N isomerization inhibition and CHEF), and the fluorescence intensity can reflect the concentration of Zn^{2+}/Cd^{2+}. The detection limits for Zn^{2+} was 0.68 μM and for Cd^{2+} was 0.94 μM, and the binding constants for Zn^{2+} was $(1.38 \pm 0.25) \times 10^6$ M^{-1} and for Cd^{2+} was $(7.49 \pm 0.18) \times 10^5$ M^{-1}. In acetonitrile solution, although the sensor **55** can reversibly (EDTA) detect Zn^{2+} and Cd^{2+}, the affinity for Zn^{2+} is stronger than that for Cd^{2+}.

In 2018, R. Purkait's research group described a multi-analyte responsive sensor **56** (Fig. 20).[13] In the DMSO/water HEPES buffer (pH = 7.2; 9 : 1, v/v) and the excitation wavelength at 482 nm, adding Zn^{2+}/Cd^{2+} enhanced the ICT effect of the sensor **56**, due to the deprotonation of the phenolic-OH of *p*-cresol moiety may facilitate charge transfer transitions. Adding Zn^{2+}/Cd^{2+}, the sensor **56** had the maximum emission at 545/
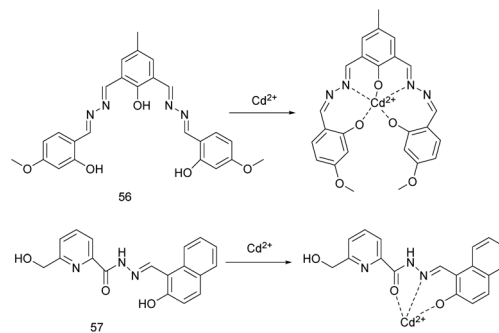

Fig. 20 Proposed binding mode of probes **56** and **57** with Cd^{2+}.

560 nm, and it emitted bright-yellow/orange fluorescence under ultraviolet light. The binding of sensor 56 to Zn^{2+} and Cd^{2+} is reversible (EDTA), the binding constants for Zn^{2+} is 2.7×10^4 M^{-1} and for Cd^{2+} is $0.96 \times 10^4 M^{-1}$, and the detection limits for Zn^{2+} is 2.7×10^{-9} M and for Cd^{2+} is 6.6×10^{-9} M, which is lower than permissible levels for these ions in drinking water by EPA. In addition, sensor 56 can detect I^- as low as 5 nM based on ESIPT. When the thin-layer chromatography plates stained with sensor 56 for field detection, Zn^{2+}, Cd^{2+}, I^- change the light red fluorescence to green, orange, and red respectively.

In 2018, N. Behera et al. reported that hydrazide probe 57 (Fig. 20).[10] Probe 57 can detect $Al^{3+}/Zn^{2+}/Cd^{2+}$ as low as 5.7×10^{-9} M/1.09×10^{-6} M/1.64×10^{-6} M in physiological pH and without Cu^{2+}, and the complexes of this probe and these metal ions can be used for detecting F^- or $H_2PO_4^-$. In MeOH–HEPES buffer solution (5 mM, pH = 7.3, 7 : 3 v/v), when excited at 435 nm, probe 57 emitted weak fluorescence at 495 nm due to the PET effect caused by electron transfer from nitrogen atom of imino (–CH=N–) group to conjugated π system of naphthalene fluorophore. Adding $Al^{3+}/Zn^{2+}/Cd^{2+}$ turned on the fluorescence of probe 57, the fluorescence intensity increased by 95/43/49 times, the emission peak shifted from 495 nm to 485/570/540 nm. But the presence of Cu^{2+} could quench the fluorescence intensity of those complexes about 20–30%. The 2 : 1 complex formed by probe 57 and Al^{3+} can detect F^- as low as 2.5×10^{-6} M by fluorescence quenching, and the 1 : 1 complex formed by probe 57 and Zn^{2+}/Cd^{2+} can detect $H_2PO_4^-$ as low as 1.43×10^{-5} M/2.11×10^{-5} M by fluorescence quenching.

A bis(salamo)-type tetraoxime sensor 58 (Fig. 21) with two N_2O_2 chelating moieties as ionophore.[5] In Tris–phosphate buffer solution (c = 0.2 M, DMF/H_2O = 9 : 1, v/v, pH = 7.0), the

change of absorbance in UV vis test shows that sensor 58 can combine with Cd^{2+}, Ni^{2+}, Zn^{2+}, and Mn^{2+}. However, only Cd^{2+} changes from faint yellow to green under 365 nm light. When the excitation wavelength at 323 nm, adding Cd^{2+} made the emission peak of sensor 58 (due to the PET inhibition and CHEF) red-shift from 412 nm to 486 nm, the fluorescence intensity increase from 125 to 712, and the fluorescence quantum yield increase from 2.6% to 13.8%. EDTA enables the sensor 58 to detect Cd^{2+} reversibly and the fluorescence emission at 373 nm can be used as a signal output to establish a molecular logic gate. In an aqueous system with a pH of 3.0 to 11.0 and a temperature of 0 to 90 °C, the sensor 58 synthesized by J. Hao's team can recognize Cd^{2+} with naked eyes (the solution changes from colorless to yellow) and fluorescence, and detect as low as 8.61×10^{-7} M without being interfered by other metal ions. The binding constant of the sensor to Cd^{2+} is as $4.98 \times 10^4 M^{-1}$. In addition, a test strip for the sensor 58 can be made to detect Cd^{2+} in food and the environment.

A phenylacetylene based sensor 59 (Fig. 21) reported by Y. Y. Zhang et al. can be used for colorimetric detection of Fe^{2+} and fluorescence proportional detection of Cd^{2+}, Zn^{2+}.[70] Adding Zn^{2+}/Cd^{2+} to the ethanol/water (1 : 1, v/v) solution of sensor 59 enhanced the electron withdrawing ability of terpyridine and enhanced the ICT effect. Upon excitation at 340 ± 5 nm, the addition of Zn^{2+}/Cd^{2+} caused the fluorescence of sensor 59 to change from blue to yellow-green/cyan, the fluorescence emission to decrease at 408 nm and to increase at 498 nm/473 nm. The fluorescence intensity ratios $F_{498 nm}/F_{408 nm}$ and $F_{473 nm}/F_{408 nm}$ were linearly related to the Zn^{2+} and Cd^{2+} concentrations, respectively. The detection limits of sensor 59 for Zn^{2+} and Cd^{2+} are 2.03×10^{-9} M and 2.62×10^{-8} M, respectively. However, Fe^{2+} can interfere the fluorescence turn on of the sensor to Zn^{2+} or Cd^{2+}. Adding Fe^{2+}, it can be observed by naked eyes that the sensor 59 solution changed from colorless to purplish red. In addition, this multifunctional sensor can be used for the detection of these ions in water samples and test strips.

Also in 2018, the M. Formica's research group synthesized probes 60a and 60b (Fig. 21).[71] The probes contain the 2,5-diphenyl[1,3,4]oxadiazole (PPD) fluorophore, methylene spacer and two coordinating units, namely dipicolylamine (DPA) for 60a and 1,4,7-triazacyclononane (TACN) for 60b. In 0.15 mol L^{-1} NMe_4Cl hydroalcoholic solution (water/ethyl alcohol 50/50 v/v), upon the excitation at 277 nm, Cd^{2+} and 60a only forms a mononuclear complex and emits high fluorescence at 368 nm. Cd^{2+} and 60b forms mononuclear and dinuclear complexes, and forms excimer to emit fluorescence at 474 nm. Probes 60a and 60b complex with Cd^{2+} at 1 : 1, with Zn^{2+} at 1 : 2 in water or hydroalcoholic medium, but the response to Zn^{2+} is not as sensitive as Cd^{2+}. Because only the mononuclear complex has a fluorescence response, so the concentration must be higher than that of the analyte when used as a sensor.

T. H. Liu and coworkers synthesized probe 61 (Fig. 22) by covalent combination of terthiophene with 2,2′:6′,2″-terpyridine.[26] In methanol solution, probe 61 forms a 2 : 1 complex with Cd^{2+}, which red-shifts the maximum absorption peak from 396 nm to 424 nm. Upon excitation at 395 nm, the fluorescence of the probe 61 changes from green to bright yellow, appears
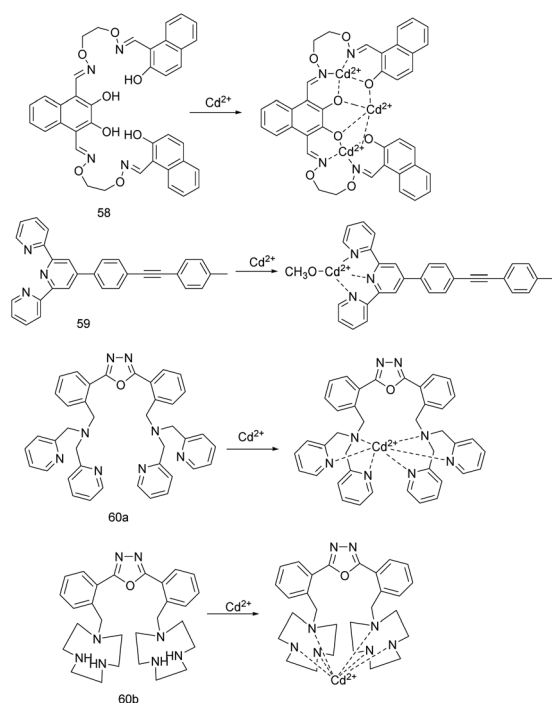

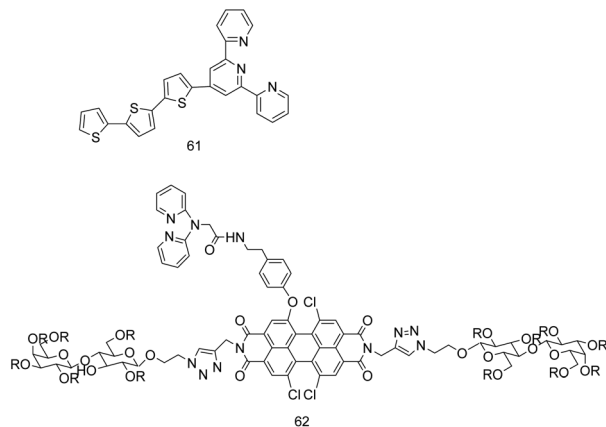Fig. 21 Proposed binding mode of probes 58 to 60 with Cd^{2+}.

Fig. 22 The structure of probes **61** and **62**.

a new emission centering at 572 nm and decreases the original emission around 504 nm. These changes can distinguish the response of this probe to other metal ions (Co^{2+}, Cu^{2+}, Ni^{2+}, Zn^{2+}, *etc.*). Probe **61** can detect Cd^{2+} in a pH environment of 5–8 as low as 1.74×10^{-7} M, and the binding constant is 2.25×10^{5} M^{-1}. Alternating addition of metal ions and EDTA can't achieve the reversibility of the fluorescence changes induced by metal ion. Cu^{2+}, Co^{2+} or Zn^{2+} not only blocks the probe **61** from forming a complex with Cd^{2+}, but also ensures the quenching of the fluorescence.

In 2019, J. K. Xiong's team reported the sensor **62** (Fig. 22) of a perylene bisimide derivative conjugated with lactose and DPA.[14] In an aqueous solution with a pH of 3.0–9.5, the sensor **62** can highly and selectively bind to Cd^{2+} in a stoichiometric ratio of 2 : 1, and the binding constant is $(6.0 \pm 0.3) \times 10^{4}$ M^{-1}. Although this sensor can detect Cd^{2+} as low as 5.2×10^{-7} M, the present of Zn^{2+}, Co^{2+} or Cu^{2+} can quench the fluorescence induced by Cd^{2+}.

P. Ravichandiran *et al.* designed probe **63** (Fig. 23) by introducing a furan-2-carboxamide group to a phenoxazine fluorophore and a phenyl sulfonyl chelating site.[72] In CH_3CN/H_2O (99 : 1, v/v) medium, when excited at 340 nm, probe **63** emitted weak fluorescence due to the C=N isomerization and ICT effects. The combination of probe **63** with Cd^{2+} strengthened the charge transfer between the secondary amine and the amide group (–CONH) of the benzoxazine moiety and enhanced the ICT effect. In addition, the use of polar organic solvent acetonitrile, these result in a 130-fold increase in the fluorescence of probe **63** at 530 nm. The binding constant is 1.36×10^{6} M^{-2}, and the detection limit for Cd^{2+} is 0.60 μM. Probe **63** recognizes Cd^{2+} with selectivity and reversibility (EDTA), and can be used for detecting Cd^{2+} in living cells. In addition, the complex of probe **63** and Cd^{2+} can turn-off the fluorescence to detect CN^{-} with a detection limit of 0.145 μM.

The research group of M. Das synthesized a pyridyl based Schiff base sensor **64** (Fig. 23).[73] In methanol solution, under excitation wavelength at 290 nm, adding Cd^{2+} and Ni^{2+} quenched the fluorescence of sensor **64**. The sensor **64** has maximum absorption at 234 nm and 272 nm, adding Cd^{2+}/Ni^{2+} led to the maximum absorption peaks red-shift from 272 nm to 280/281 nm, and the interference of other metal ions and anions was neglected. The binding constants of sensor **64** to Cd^{2+} and Ni^{2+} were 4.29×10^{6} L mol^{-1} and 26.88×10^{6} L mol^{-1} calculated by Yoe Jones method, respectively. The detection limit for Cd^{2+} was 1.4688 μM, and for Ni^{2+} was 3.08 μM.

M. Vera *et al.* designed sensor **65** (Fig. 23).[29] They inserted –CH_2– between the DTPA (diethylenetriaminepentaacetate) and the naphthalene chromophore to make the complex stable and have little impact on the environment when Cd^{2+} was detected by sensor **65**. Furthermore, sensor **65** can distinguish Zn^{2+} and Cd^{2+}, and without fluorescence quenching caused by paramagnetic effect. In an aqueous solution and the excitation wavelength at 280 nm, sensor **65** has strong naphthalene-monomer emission at 355 nm and excimer emission at 410 nm. The sensor **65** is coordinated with Cd^{2+}, so that the fluorescence emission of excimer is increased by 70–100%, while the monomer emission is hardly affected. The sensor **65** is coordinated with Zn^{2+}, so that the fluorescence emission of excimer is decreased by 60%, while the monomer emission is increased.

P. Kaur's research group synthesized a 1,2,3-triazole linked fluorescein derivative probe **66** (Fig. 24).[30] In an ethanol/water (4 : 1, v/v) solution, probe **66** has high selectivity to Cd^{2+} and Co^{2+}. It binds to Cd^{2+} and Co^{2+} through the N, O, N cornered caged of probe **66**. Due to the PET effect, probe **66** shows fluorescence turn off for Cd^{2+} and fluorescence turn on for Co^{2+}, and the detection limits at 9–10 μM.

Using 2,9-dimethyl-1,10-phenanthroline and *o*-aminophenol as raw materials, M. X. Huang *et al.* synthesized a simple, sensitive and practical fluorescence enhanced probe **67** (Fig. 24) for Cd^{2+}.[74] The performance of probe **67** to recognize Cd^{2+} was tested in DMF–water (v/v, 3 : 7) solution, excitation wavelength at 275 nm, and emission wavelength at 377 nm. The addition of Cd^{2+} restricted the PET process (electron transfer from the N of imine to phenanthroline ring) and the C=N isomerization, resulting in charge rearrangement and rigidity enhancement. Therefore, Cd^{2+} led to fluorescence enhancement and
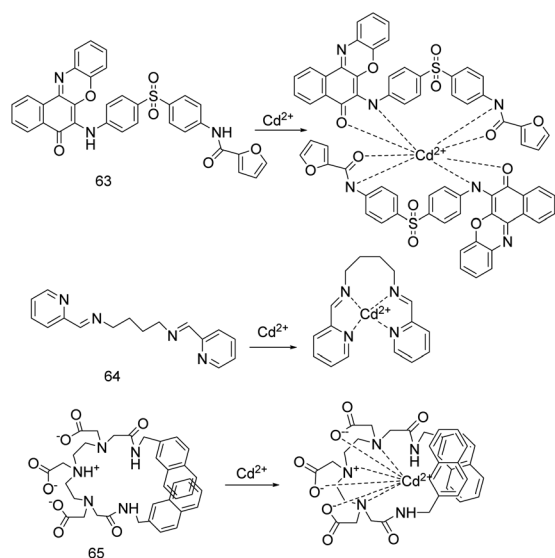

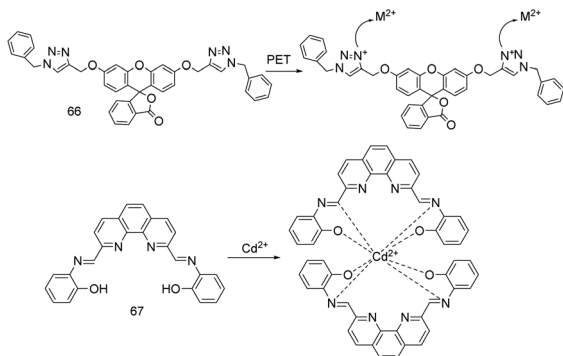Fig. 23 Proposed binding mode of probes **63** to **65** with Cd^{2+}.

Fig. 24   Proposed sensing mode of probes **66** and **67** with Cd^{2+}.

fluorescence lifetime reduction of the probe **67**. The binding constant between the probe **67** and Cd^{2+} is 3.15×10^5 M^{-1}. The emission intensity of probe **67** at 377 nm has a good linear relationship with Cd^{2+} at 0.025–2.5 μM, and it can be quantitatively detected as low as 29.3 nM. Cd^{2+} can enhance the fluorescence of probe **67** in 6.6 s, but its same group elements Cu^{2+} and Pb^{2+} can quench the fluorescence induced by Cd^{2+} to some extent. The researchers not only proposed the binding method of the probe **67** and Cd^{2+} by Job plot, FT-IR and ^{1}H NMR titration experiments, but also confirmed the accuracy of the probe in the detection of Cd^{2+} by the determination of Cd^{2+} in different water samples.

The probe **68** (Fig. 25), which was designed by conjugation of terpydine (a receptor for Zn^{2+} and Cd^{2+}) and pyridinium with the styryl group, has good selectivity and anti-interference ability for Cd^{2+} recognition.[75] Probe **68** responds to Cd^{2+} based on the ICT and AIE mechanisms. In $DMSO/H_2O$ system, upon excitation at 375 nm, the energy consumed by the intramolecular rotation of multiple pyridinium rings made the probe **68** emit weak fluorescence. As the water fraction in the solution increases to more than 80%, molecules aggregation and inhibition of intramolecular rotation made the probe **68** emit bright fluorescence. Adding Cd^{2+} made the fluorescence emission peak of the probe **68** red shift from 480 nm to 530 nm, but adding Zn^{2+} did not emerge obvious fluorescence spectral changes. W. X. Lin et al. introduced pyridinium group and alkane with sixteen carbon atoms into the probe **68** to increase its water solubility and cell membrane permeability, which can be used to detect and label Cd^{2+} in cells.[75]

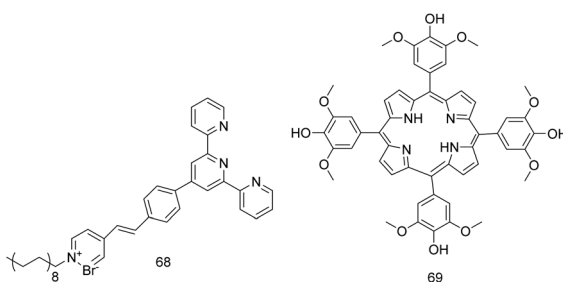The next year, P. P. Namitha's study team reported sensor **69** (Fig. 25).[76] In an ethanol solution and the excitation wavelength at 427 nm, the strong fluorescence of sensor **69** was quenched by Cd^{2+} due to the PET effect, and the fluorescence intensity ratio I_0/I has a linear relationship with Cd^{2+} of 0.25–2 μM. Ni^{2+}, Zn^{2+} and Cu^{2+} can interfere with Cd^{2+} detection when the concentration exceeds 10 times of Cd^{2+} concentration, and when they exceed 100 times, they can slightly quench the fluorescence caused by Cd^{2+}. The sensor **69** can detect Cd^{2+} as low as 0.1499 μM with excellent selectivity, light stability and water solubility, and can be used to measure Cd^{2+} in the NIR region.

In 2020, P. Liu et al. reported a fluorescent probe **70** (Fig. 26) based on ICT to detect Cd^{2+}.[77] In HEPES buffer (1% DMSO as cosolvent) and the excitation wavelength at 380 nm, probe **70** has no colour and fluorescence response to cations other than Cd^{2+}. The addition of Cd^{2+} turns the yellow weak fluorescence of probe **70** into red strong fluorescence, and the fluorescence intensity is linearly related to the Cd^{2+} concentration of 5.0×10^{-8} to 5.0×10^{-5} mol L^{-1}. The association constant between probe and Cd^{2+} was 7.97×10^4 M^{-1}, and the detection limit for Cd^{2+} was 6.31 nM. In addition, the probe solution changes from yellow to maroon red by adding Cd^{2+}, so it can be used as a new visual sensor for Cd^{2+}. The probe **70** is easy to synthesize, and has excellent selectivity, sensitivity, reversibility (EDTA), stability, and a wide pH (3–13) range for Cd^{2+} detection. In addition, the probe **70** can be used for fluorescence imaging of Cd^{2+} in living cells.

The sensor **71** (Fig. 26) designed by B. Jana's research team has high response efficiency to Cd^{2+} in water medium with pH of 1–10 and lower temperature.[78] In aqueous medium (water/DMSO, v/v: 95/5), sensor **71** has maximum absorption at 367 nm and 293 nm, the addition of Cd^{2+} makes maximum absorption shift from 293 nm to 313 nm. Under 367 nm, the addition of Cd^{2+} increases the fluorescence emission intensity of sensor **71** at 482 nm by 3 times, the fluorescence lifetime increases from 6.49 ns to 9.78 ns, and the fluorescence changes from colorless to faint blue. The dissociation constant (K_d) of Cd^{2+} and probe complex is 1.7×10^{-7}, and the detection limit for Cd^{2+} is 0.95 μM. The fluorescence intensity ($F_0/(F-F_0)$) and Cd^{2+} ($1/[Cd^{2+}]$) with a concentration of 0.05–1 μM has a linear relationship, which can be used to quantitatively detect Cd^{2+}. However, the presence of Hg^{2+} can be reduced the fluorescence intensity of the complex by 9–10%.
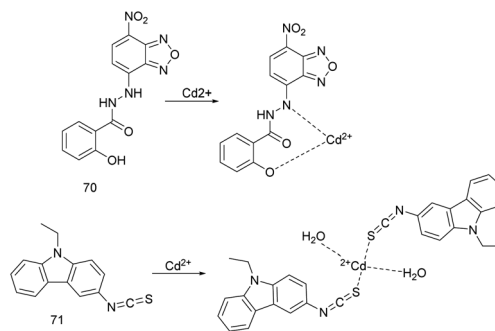

Fig. 25   The structure of probes **68** and **69**.

Fig. 26   Proposed binding mode of probes **70** and **71** with Cd^{2+}.

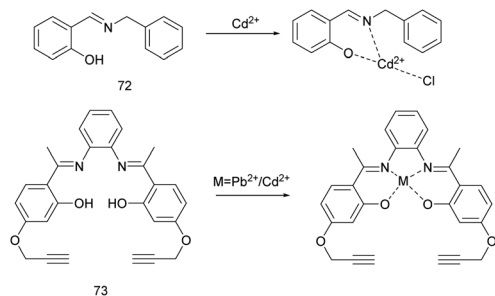**Fig. 27** Proposed binding mode of probes **72** and **73** with Cd^{2+}.

Fig. 28 Proposed binding mode of probes **74** to **76** with Cd^{2+}.

In 2020, E. K. Inal *et al.* reported the sensor **72** (Fig. 27).[79] The ethanol–water solutions and the excitation wavelength at 369 nm are selected to carry out. The sensor **72** emits weak fluorescence at 464 nm, then addition of $Zn^{2+}/Cd^{2+}/Hg^{2+}$ makes the sensor has obvious fluorescence emission at 452/474/491 nm, the fluorescence intensity and $Zn^{2+}/Cd^{2+}/Hg^{2+}$ concentration has a linear relationship. The detection limit for $Zn^{2+}/Cd^{2+}/Hg^{2+}$ is 2.7×10^{-7} M/6.0×10^{-7} M/7.5×10^{-7} M. The sensor **72** can detect Zn^{2+}, Cd^{2+}, Hg^{2+} in ethanol–water solutions with a pH of 8–9 (due to the protonation of nitrogen in imine bond, the fluorescence response to metal ions in acidic medium is very weak), but the sensor has a stronger affinity for Cu^{2+} and Fe^{3+}. Moreover, Co^{2+} and Ni^{2+} interferes with the selectivity of the sensor **72** for Zn^{2+} and Cd^{2+}.

The research group of S. G. J. Andrews reported probe **73** (Fig. 27).[80] The coordination of probe **73** with Cd^{2+} or Pb^{2+} led to inhibit the PET process and produce the CHEF effect, so probe **73** emitted strong fluorescence. Probe **73** has selectivity, sensitivity, reversibility (EDTA) and visualization for the recognition of Cd^{2+} and Pb^{2+} in an aqueous buffer (<80%) medium, and is not affected by other metal ions or interferes with each other. In methanol/HEPES buffer (5 mM, v/v = 1 : 9, pH = 7.3), upon excitation at 420 nm, adding Cd^{2+} makes the emission peak of probe **73** redshift from 553 nm to 578 nm, and can detect Cd^{2+} as low as 12.96 nM in a pH system of 4.8–8.5. Upon excitation at 410 nm, adding Pb^{2+} makes the emission peak of probe **73** redshift from 499 nm to 505 nm, and can detect Pb^{2+} as low as 10.63 nM in a pH system of 5.0–8.4. The binding constants of probe for Cd^{2+} is 3.10×10^{5} M^{-1} and for Pb^{2+} is 2.40×10^{5} M^{-1}. The probe **73** can be used as a naked-eye sensing probe for Cd^{2+} and Pb^{2+}. Under visible light, the solution of the probe **73** changes from pale yellow to dark yellow and light pink, respectively. Under ultraviolet light, the probe solution changes from pale yellow to green and red, respectively. In addition, probe **73** can be used for fluorescence imaging of Cd^{2+} and Pb^{2+} in MCF 7 cells.

Y. F. Zhang *et al.* synthesized the sensor **74** (Fig. 28) by connecting 2-(2-((2-hydroxyphenyl)imino)ethylidene)amino unit (as the recognition site of Pb^{2+} and Cd^{2+}) and *tert*-butyldiphenylsilyl (as the reaction center of F^-, and improving the stability of the probe molecule and protecting the molecule from modification) to fluoresceins.[81] Sensor **74** can recognize Pb^{2+} and Cd^{2+} quickly and sensitively by using F^- as auxiliary reagent. In EtOH/H_2O (99 : 1, v/v) sensor solution, adding Pb^{2+}

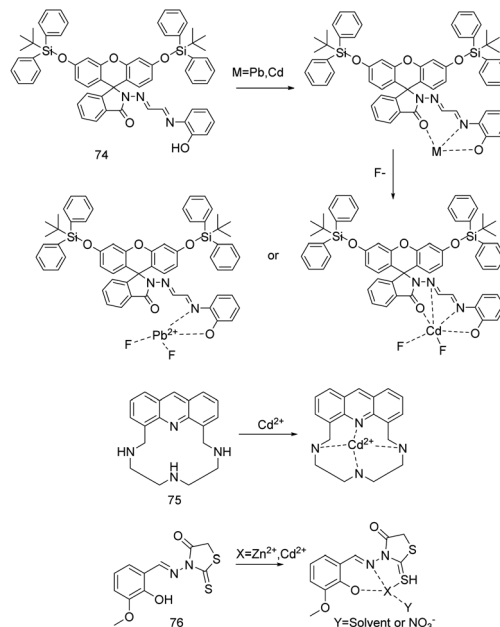or Cd^{2+} increased the absorption band at 533 nm and decreased the absorption band at 374 nm, resulting in the change of ratiometric spectral. When F^- is added to the sensor solution containing Pb^{2+} or Cd^{2+}, the solution containing Pb^{2+} fades from light purple to colorless, and the solution containing Cd^{2+} deepens from light purple to dark purple. Through these phenomena, this sensor can be used as an indirect sensor to identify F^-. The researchers believe that these phenomena are caused by the different radius of Pb^{2+} and Cd^{2+} and the different coordination mode with F^-. The binding constants (K_a) of the sensor **74** with Pb^{2+} or Cd^{2+} are 3.292×10^{4} M^{-1} and 2.349×10^{4} M^{-1}, respectively. The detection limits of sensor **74** for Pb^{2+} and Cd^{2+} are 0.42 μM and 0.53 μM, respectively.

F. D. Carlos' team has developed an acridine based fluorophore sensor **75** (Fig. 28).[82] In EtOH : CH_3Cl (99 : 1 v/v) solution, the combination of sensor **75** with Cd^{2+} suppressed the PET effect and enhanced the fluorescence. Under the excitation of 400 nm light, the fluorescence intensity of sensor **75** was enhanced by 746% with the addition of Cd^{2+}, and was not affected by interference ions. The linear range of fluorescence intensity and Cd^{2+} concentration was 0.10–1.00 μmol L^{-1}. The binding constant of sensor **75** to Cd^{2+} is 1.05×10^{9} L mol^{-1}, and the detection limit and quantitative detection limit are 9.98 and 33.31 nmol L^{-1}, respectively. Sensor **75** has repeatability, reproducibility, robustness and reversibility (EDTA) for detecting Cd^{2+}. In addition, sensor **75** can be used to detect Cd^{2+} in Brazilian sugarcane wine and tobacco smoke extract.

Rhodanine and salicylidene Schiff bases can bind to metal ions strongly, and have good photophysical properties and water solubility.[83] Therefore, the probe **76** (Fig. 28) was designed and synthesized by S. Park *et al.* When probe **76** was used to detect Zn^{2+} or Cd^{2+} in aqueous medium ($\lambda_{ex} = 329$ nm), the fluorescence intensity at 519 nm increased significantly.[83]
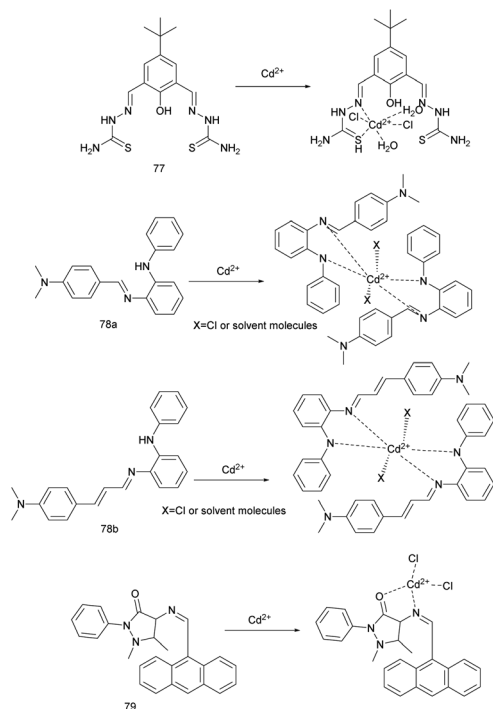

Fig. 29 Proposed binding mode of probes **77** to **79** with Cd^{2+}.

However, the addition of cysteine can make the fluorescence induced by Cd^{2+} disappear, while the fluorescence induced by Zn^{2+} remain, so the distinction between Zn^{2+} and Cd^{2+} is realized. The binding constant of probe to Zn^{2+} or Cd^{2+} is 2.0×10^7 M^{-1} or 1.0×10^7 M^{-1}, and the detection limit for Zn^{2+} or Cd^{2+} is 1.07 μM or 1.37 μM. The probe **76** can respond to Zn^{2+} (detection is affected by Co^{2+}, Cu^{2+}, Fe^{3+}, Fe^{2+}, Na^+) or Cd^{2+} (detection is affected by Co^{2+}, Cu^{2+}, Fe^{3+}, Fe^{2+}, Na^+, Zn^{2+}) in the pH range of 7.0–9.0 for water sample analysis and cell imaging, but its anti-interference ability is poor.

Because thiosemicarbazide has many coordination modes with metal ions, P. S. Kumar *et al.* synthesized the probe **77** (Fig. 29) by connecting it to the fluorophore unit (4-*tert*-butyl-2,6-diformylphenol).[84] The probe can be used for the fluorescence detection of Zn^{2+}, Cd^{2+} and Hg^{2+} in H_2O : DMSO (95 : 5 v/v) medium and 360 nm excitation wavelength. The fluorescence intensity ratios $I_{488\ nm}/I_{540\ nm}$ and $I_{470\ nm}/I_{540\ nm}$ were linearly correlated with the concentrations of Zn^{2+} and Cd^{2+}, respectively. Hg^{2+} makes the probe emit weak reddish brown fluorescence near 578 nm. The binding constants of Zn^{2+}, Cd^{2+} and Hg^{2+} complexes are 9.8×10^3, 1.39×10^5 and 2.03×10^{13} M^{-1}, respectively. The binding ability of the probe to Zn^{2+}, Cd^{2+} and Hg^{2+} increased in turn, and the metal ions with strong binding ability could interfere with the detection of metal ions with weak binding ability. Probe **77** can respond to Zn^{2+}, Cd^{2+} and Hg^{2+} in the pH range of 3–10, with detection limits as low as 5.1, 3.4 and 0.51 μM.

Z. Aydin *et al.* reported the Schiff base probes **78a** and **78b** (Fig. 29) with *N*-phenyl-*o*-phenylenediamine as Cd^{2+} binding part and benzaldehyde and cinnamaldehyde as chromophores.[85] For the recognition of Cd^{2+} ions in aqueous solution,

the probe **78a** changes from colorless to orange, and the probe **78b** changes from yellow to reddish. These probes can quantitatively detect Cd^{2+} based on absorbance. Although the ions has no effect on the colorimetric detection of Cd^{2+} by **78b**, its spectrometric titration is interfered by Zn^{2+}. The binding constants of **78a** and **78b** with Cd^{2+} were 2.65×10^{12} M^{-2} and 4.95×10^{12} M^{-2}, respectively. The detection limits of **78a** and **78b** were 4.38×10^{-7} M and 1.02×10^{-7} M, respectively. The two probes have selectivity and reversibility for the recognition of Cd^{2+}, and can be used as colorimetric sensors for the detection of Cd^{2+} in aqueous solution.

J. J. Celestina *et al.* rapidly synthesized the colorimetric and fluorescent sensor **79** (Fig. 29) for Cd^{2+} from 4- aminoantipyrine and 9-anthracene carboxaldehyde under microwave irradiation.[86] The addition of Cd^{2+} makes the sensor produce PET-CHEF effects and inhibit the C=N isomerization, resulting in the solution changes from yellow to light brown and the fluorescence changes from yellow to green. The detection limit of the sensor **79** for Cd^{2+} is as low as 0.02 μM, and the detection is reversible and specific. In addition, sensor **79** can be used for the detection of Cd^{2+} in water samples and fluorescence imaging in L929 cells.

P. Lasitha *et al.* synthesized a squaramine ring based probe **80** (Fig. 30), which can respond to Zn^{2+} and Cd^{2+} by turning on fluorescence.[87] Under the excitation of 400 nm light, the maximum emission peak of the probe shifts from 464 nm to long wavelength with the addition of $Zn(CH_3COO)_2$ and $Cd(CH_3COO)_2$. With the addition of $Zn(CH_3COO)_2$, a new emission band appeared at 560 nm, and gradually red shifted to 595 nm. Similarly, with the addition of $Cd(CH_3COO)_2$, a new emission band appeared near 530 nm, and gradually red shifted to 540 nm. The order of stokes shift emission is the same as that of anion basicity ($ClO_4^- < Cl^- < NO_3^- < SO_4^{2-} < CH_3COO^-$). The detection limits for $Zn(CH_3COO)_2$ and $Cd(CH_3COO)_2$ were 5×10^{-7} M (32.6 ppb) and 7×10^{-8} M (7.8 ppb), respectively.

M. Muddassir's team prepared a complex sensor **81** (Fig. 30) of 3,5-dimethylpyrazole with Cu^{2+} perchlorate.[88] Sensor **81** can identify Cd^{2+} in aqueous solution by fluorescence enhancement, and is not interfered by other metal ions. M. Muddassir *et al.* confirmed the binding of the complex with Cd^{2+} by X-ray photoelectron spectroscopy (XPS) analysis.[88] They speculate
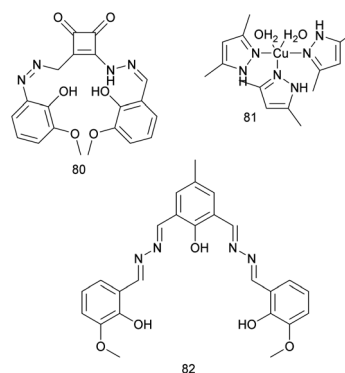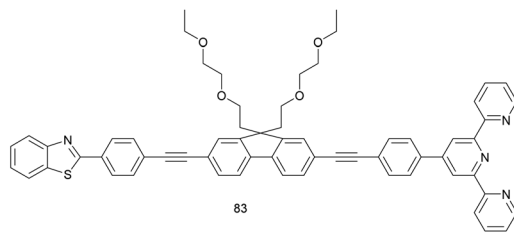

Fig. 30 The structure of probes **80** to **82**.

Fig. 31 The structure of probe **83**.

that the high selectivity and sensitivity to Cd^{2+} may be due to the interaction between Cd^{2+} and 3,5-dimetylpyrazole ligand through Lewis acid–base interactions, which promotes more effective energy transfer from ligand to Cu^{2+}. In addition, the complex probe can also respond to acetone by fluorescence quenching.

Vanillinyl-hydrazone Schiff base probe **82** (Fig. 30) is a turn-on fluorescent probe for Mg^{2+}, Zn^{2+}, Cd^{2+} and I^-, which was reported by S. Dey's team in 2020.[89] In DMSO/H_2O medium (9 : 1) and under 480 nm excitation wavelength, the different emission wavelengths and fluorescence colors of this probe can be used as the methods to distinguish Zn^{2+} (λ_{em} = 546 nm, yellow green), Cd^{2+} (λ_{em} = 576 nm, yellow) and Mg^{2+} (λ_{em} = 625 nm, orange). The binding constants of probe **82** to Zn^{2+}, Cd^{2+} and Mg^{2+} are 8.07×10^4 M^{-1}, 6.5×10^4 M^{-1} and 4.38×10^4 M^{-1}, respectively. The detection limits for Zn^{2+}, Cd^{2+} and Mg^{2+} were 14×10^{-9} M, 6.8×10^{-9} M and 11.5×10^{-9} M, respectively. In different detection environments, probe **82** can also be used as a fluorescent probe for I^-, and the detection limit is as low as 5.9 nM.

Using fluorene as fluorophore, 2,2′,6′,2″-terpyridine as ligand and benzothiazole as electron acceptor, D. Yue *et al.* synthesized probe **83** (Fig. 31) with high electron absorption, fluorescence quantum yield and photostability.[90] They also introduced 2-(2-ethoxyethoxy)-ethyl group to enhance the solubility of the probe. Zn^{2+} and Cd^{2+} were identified by different emission colors in acetonitrile. The detection limits for Zn^{2+} and Cd^{2+} were 11.25 nM and 1.80 nM, respectively.

The spectroscopic and analytical parameters of other Cd^{2+} sensors based on small organic molecules are listed in Table 7. There are many problems in these probes, such as low sensitivity, poor water solubility and weak anti-interference ability. Some probes recognize Cd^{2+} only through colorimetric response, and they generally have high selectivity and anti-interference, but their sensitivity is not high (the minimum detection limit is 102 nM). Fluorescent sensors usually have high sensitivity, but in these reports, there are relatively a few sensors with detection limits as low as 10^{-7} M. Few sensors can meet the requirements of water solubility, selectivity, sensitivity, anti-interference and practicability (such as appropriate pH, temperature and response time).

9. Nanosensor-based Cd^{2+} fluorescent sensor

Compared with small organic molecules fluorescent probes, the nanosensor-based fluorescent and colorimetric probes on avoid

complex synthesis and purification processes.[91] In addition, nanosensors have the characteristics of wide excitation wavelength, adjustable size, high quantum yield and good photochemical stability.[91,92] Therefore, the development of nanosensors in Cd^{2+} fluorescent probes is also worthy of our attention.

In 2017, Q. Wu's team first reported a probe **84** that enhances the fluorescence of the second near-infrared (NIR-II) region based on quantum dots identification Zn^{2+} and Cd^{2+}.[93] The research group prepared oil-soluble Ag_2S QDs by capping Ag_2S nanocrystals with *n*-dodecyl mercaptan groups. However, due to the limited application of the oil-soluble probe, they replaced dodecyl mercaptan as a surface ligand with thioglycollic acid containing carboxyl group to obtain water-soluble probe **84**. The UV-vis absorption spectrum of probe **84** has no obvious peak in the range of 250–910 nm, and the fluorescence emission intensity gradually decreases with the increase of excitation wavelength. After adding Zn^{2+} or Cd^{2+}, thioglycollic acid on the surface of probe **84** reacts with ions to form Zn–thiol or Cd–thiol complex passivation shell around the surface of Ag_2S quantum dots. Due to the passivation shell repairing surface defects and inhibiting non-radiative recombination pathway, the fluorescence intensity of probe **84** at 1100 nm increased by 7 or 8.5 times under 480 nm light excitation, and the fluorescence lifetime increased from 3.25 ns to 7.35 or 10.42 ns, respectively. The fluorescence intensity ratio (I/I_0) of probe **84** has a linear relationship with the concentration (1–40 μM) of Zn^{2+} or Cd^{2+}, and can be used for quantitative detection of Zn^{2+} or Cd^{2+}. The detection limits of probe **84** for Zn^{2+} and Cd^{2+} are 760 nM and 546 nM, respectively. In addition, the probe **84** has strong practicability. It can not only detect Zn^{2+} or Cd^{2+} in lake water and tap water samples, but also be used for cell imaging of Zn^{2+} in NIR-II region.

According to the interaction between C=N group and specific metal ions, J. T. Wang *et al.* obtained 3D porous MOF-UiO-66-N=CH$_2$ with perfect octahedral morphology and particle size of about 100 nm through the interaction of –NH$_2$ of UiO-66-NH$_2$ with formaldehyde.[94] MOF-UiO-66-N=CH$_2$ was used as the fluorescent probe **85** of Cd^{2+}. In aqueous solution and light excitation at 342 nm, probe **85** has an emission peak at 468 nm. When metal ions were added to probe **85**, only Fe^{3+} quenched its fluorescence intensity, Cd^{2+} and Zn^{2+} increased its fluorescence intensity, and the effects of other metal ions could be neglected. However, the increase of luminescence intensity of probe **85** caused by Cd^{2+} is the strongest, and the fluorescence intensity ratio (I/I_0) has a good linear relationship with Cd^{2+} concentration (0–500 μM). Therefore, probe **85** can be used as a fluorescence on probe for quantitative detection of Cd^{2+}, the detection limit is as low as 0.336 μM (37.8 ppb), and the K_{SV} value is 3.81×10^3 M^{-1}. In addition, probe **85** has low-toxicity and pH (4–10) independence, and is promising for Cd^{2+} detection in water and intracellular environments.

In 2017, L. Li's research team reported a fluorescent probe **86** based on dithizone (DZ) etched cadmium telluride nanoparticles (CdTe NPs) for the detection of Cd^{2+}.[92] After DZ was added to L-cysteine-capped CdTe NPs, the Cd–thiol complex surface layers was destroyed and the surface passivation was

Table 7 Spectroscopic and analytical parameters of other small organic molecules based Cd^{2+} fluorescent and colorimetric probes

Probe	Solvent	Excitation wavelength (nm)	Emission wavelength (nm) λ_{em_0}–λ_{em}	Detection limit (nM)	Association constant	Interfering ion(s)	Ref.
44	CH_3CN–H_2O (1:5)	400	558–561	10.21	3.16×10^5 M^{-1}	—	12
45	CH_3CN	410; 495	675–570; 730–570	6.9	—	Zn^{2+}	19
46	H_2O	418	653–611	32	$K_d = 31.2 \pm 5.2$ μM	Hg^{2+}, Cu^{2+}	60
47	EtOH–H_2O (9:1)	470	545–537	57.6	—	Many	17
48	NPA/CYH (1:30)	495	518–538	2	—	Co^{2+}, Cu^{2+}, Zn^{2+}, Hg^{2+}	61
49	DMF	—	—	200	3.7×10^4 M^{-1}	—	62
50	EtOH – EAC (7:3)	283	510	2690	—	—	63
51	CH_3CN–H_2O (1:99)	315	433	100	3862.872 M^{-1}	—	64
52	MeOH	308	450	50	$K_b = 4.87$	IO_4^-, Zn^{2+}	66
53a/b	DMSO; DMF	—	—	3220; 200	—	—; Hg^{2+}, Cu^{2+}, Pb^{2+}	67
54	MeOH	320	418–393	1020	—	Al^{3+}	68
55	CH_3CN	378	452	940	$(7.49 \pm 0.18) \times 10^5$ M^{-1}	Zn^{2+}	69
56	DMSO–H_2O (9:1)	482	560	6.6	0.96×10^4 M^{-1}	Zn^{2+}, I^-	13
57	MeOH–H_2O (7:3)	435	495–540	1640	—	Cu^{2+}	10
58	DMF–H_2O (9:1)	323	412–486	861	4.98×10^4 M^{-1}	—	5
59	EtOH–H_2O (1:1)	340	473	26.2	—	Fe^{2+}	70
60a/b	EtOH–H_2O (1:1)	277	368/474	—	—	—	71
61	MeOH	395	572	174	—	Cu^{2+}, Co^{2+}, Zn^{2+}	26
62	H_2O	528	600	520	$(6.0 \pm 0.3) \times 10^4$ M^{-1}	Zn^{2+}, Co^{2+}, Cu^{2+}	14
63	CH_3CN–H_2O (99:1)	340	530	600	1.36×10^6 M^{-2}	CN^-	72
64	MeOH	—	—	14 688	4.29×10^6 M^{-1}	—	73
65	H_2O	280	355/410	—	—	Zn^{2+}	29
66	EtOH–H_2O (4:1)	—	—	9000–10 000	—	Co^{2+}	30
67	DMF–H_2O (3:7)	275	377	29.3	3.15×10^5 M^{-1}	Cu^{2+}, Pb^{2+}	74
68	DMSO–H_2O	375	480–530	—	—	Fe^{3+}, Co^{2+}, Cu^{2+}, Pb^{2+}	75
69	EtOH	427	656	149.9	—	Ni^{2+}, Zn^{2+}, Cu^{2+}	76
70	DMSO–H_2O (9:1)	380	513–515	6.31	7.97×10^4 M^{-1}	—	77
71	DMSO–H_2O (5:99)	367	482	950	$K_d = 1.7 \times 10^{-7}$	Hg^{2+}	78
72	EtOH–H_2O	369	464–474	600	—	Cu^{2+}, Fe^{3+}, Co^{2+}, Ni^{2+}	79
73	MeOH–H_2O (1:9)	420	553–578	12.96	3.10×10^5 M^{-1}	Pb^{2+}	80
74	EtOH–H_2O (99:1)	—	—	530	2.349×10^4 M^{-1}	Pb^{2+}	81
75	EtOH–CH_3Cl (99:1)	400	416	9.98	1.05×10^9 L mol^{-1}	—	82
76	H_2O	329	519	1370	1.0×10^7 M^{-1}	Co^{2+}, Cu^{2+}, Fe^{3+}, Fe^{2+}, Na^+, Zn^{2+}	83
77	DMSO–H_2O (5:99)	360	578	3400	1.39×10^5 M^{-1}	Zn^{2+}, Hg^{2+}	84
78a/b	H_2O	—	—	438/102	2.65×10^{12} M^{-2}/4.95×10^{12} M^{-2}	—	85
79	EtOH	398	345–404 and 465	20	—	Many	86
80	DMSO	400	530–540	70	—	Zn^{2+}	87
81	CH_3CN–H_2O	267	650	—	—	—	88
82	DMSO–H_2O (9:1)	480	576	6.8	6.5×10^4 M^{-1}	Zn^{2+}, Mg^{2+}, I^-	89
83	CH_3CN	410	460	1.8	—	Zn^{2+}	90

reduced due to the chemical etching effect of DZ, resulting in the reduction of fluorescence intensity and fluorescence lifetime. After adding Cd^{2+} to the weakly fluorescent CdTe NPs–DZ mixture (probe 86), the recognition site of Cd^{2+} on the surface of NPs can selectively bind Cd^{2+} to re-passivate the surface of NPs, resulting in the increase of fluorescence intensity and fluorescence lifetime. Under ultrapure water medium and excitation wavelength of 328 ± 5 nm, DZ or Cd^{2+} can be quantitatively detected within 40 min according to the fluorescence intensity (468 nm) ratio before and after adding DZ or Cd^{2+}. The detection limit for DZ is 2.7 μM, and the detection limit for Cd^{2+} is 0.13 μM. In addition, Ag^+ and Cu^{2+} almost completely quench the fluorescence of non-etched and DZ etched NPs. However, thiourea can be selected as a masking agent to eliminate the interference of Ag^+ and Cu^{2+}.

In 2017, Y. Yang et al. reported a super stable Eu-MOF luminescent probe 87. The probe 87 has extremely high thermal stability, air stability and chemical stability, and has fluorescence response to multiple analytes.[95] The luminescence sensing of metal ions by probe 87 was studied in aqueous solution and 324 nm excitation wavelength. It was found that the fluorescence intensity of probe 87 at 613 nm gradually increased (2.18 times)/decreased (about 85%) with the addition of Cd^{2+}/Mn^{2+}. According to Stern–Volmer (SV) equation: $I_0/I = 1 + K_{SV}[M]$, the quenching effect coefficients (K_{SV}) of probe 87 for Cd^{2+} and Mn^{2+} are -54 or 443 L mol^{-1} respectively, indicating that Mn^{2+} has high fluorescence quenching efficiency for probe 87. Probe 87 can detect Cd^{2+} and Mn^{2+} as low as 10^{-6} M. The research team speculated that the increase or quenching of fluorescence of probe 87 caused by Cd^{2+}/Mn^{2+} may be due to the

cation exchange between free $[Me_2NH_2]^+$ and target ions and the interaction between metal ions and organic ligands. In addition, methanol or ether can significantly enhance or weaken the emission of probe **87** at 613 nm, which is the first time to use Ln-MOFs as a luminescent probe to identify ether molecules.

Because biomass contains a lot of carbohydrates, it can be used as raw material for preparing carbon dots (CDs). In 2018, D. Gu's team synthesized a nitrogen and sulfur co-doped sensor **88** with scallion as carbon source, which can detect Cd^{2+} by fluorescence quenching.[96] The response of sensor **88** to Cd^{2+} was studied in HAC–NaAc buffer solution (pH = 5.0) and 390 nm excitation wavelength. The linear relationship can be established between the emission intensity ratio of sensor **88** at 455 nm and Cd^{2+} concentration of 0.1–3.0 μM or 5.0–30.0 μM respectively, and the corresponding binding constants were $2.816 \times 10^5 \pm 11\,670$ L mol^{-1} or $3.636 \times 10^4 \pm 2120$ L mol^{-1} respectively. The sensor **88** has no obvious fluorescence response to other metal ions except Cd^{2+}, and the fluorescence quenched by Cd^{2+} is hardly disturbed by other metal ions. It can detect Cd^{2+} as low as 15.0 nM. In addition, the sensor **88** has extremely low cytotoxicity and detection limit, and has a good application prospect for Cd^{2+} ion sensing and biological imaging *in vivo* or *in vitro*.

Y. A. Pan *et al.* selected a semi-rigid ligand with carboxyl group (2,5-bis(phenylamino)-1,4-benzenedicar boxylic acid, **L**) as an aromatic organic linker and selected Zn^{2+} ions with outer shell electronic configuration similar to Cd^{2+} as ion exchange interaction sites to construct a new three-dimensional Zn-MOF sensor **89**.[97] Since Cd^{2+} replaces Zn^{2+} and reacts with the carboxyl group of **L**, a more stable Zn–Cd-MOF structure is obtained, which limits the rotation of **L** in sensor **89** and improves the rigidity of the whole system, the fluorescence of probe **89** increases when identifying Cd^{2+}. Under 365 nm UV irradiation, it can be seen that the probe **89** turns on yellow fluorescence induced by Cd^{2+}. When excited at 333 ± 5 nm, probe **89** has a fluorescence emission peak at 529 nm. After adding Al^{3+} and Cd^{2+} ions, the fluorescence emission of probe **89** is enhanced, but Al^{3+} causes the emission peak of probe **89** to red-shift to 555 nm without interfering with the quantitative detection of Cd^{2+} at 529 nm according to the fluorescence intensity ratio I/I_0. The fluorescence of probe **89** is stable within 20 min after adding Cd^{2+}, and the presence of Cu^{2+}, Mn^{2+}, Ni^{2+} and Co^{2+} in the detection system will have a slight impact on the determination of Cd^{2+}. In addition, the probe **89** can recognize nitrobenzene by fluorescence quenching, and the detection limit is 1.19 μg mL^{-1}.

Z. Y. Zhang's research team reported a graphite-like nitride doped carbon quantum dots-capped gold nanoparticle (Au@g-CNQDs, probe **90**).[98] Because the surface of probe **90** has numerous heptazine, carboxyl and hydroxyl groups, a trace amount of Cd^{2+} ions can be adsorbed on the probe **90** surface through "cooperative effect". In Tris–HCl buffer solution, the color of probe **90** changes from wine-red to blue-violet within 30 s after the addition of Cd^{2+}, and the absorption peak of probe **90** decreases at 520 nm and appears at 650 nm. The absorption ratio ($A_{650\,nm}/A_{520\,nm}$) of probe **90** has a linear relationship with Cd^{2+} concentration (0.01–3.0 μM), and Cd^{2+} can be detected

quantitatively with a detection limit of 10 nM. In addition, the probe **90** can accurately and quickly detect the distribution of Cd^{2+} ions in mouse organs and tissues, indicating that it has considerable application potential in practical application and clinical detection.

Through the reaction of chelidamic acid-picolylamine (CP) substituted diacetylene monomer and the reaction between 10,12-pentacosadiynoic acid and CP chelating part, P. Thanh Chung *et al.* synthesized probe **91** based on conjugated polyacetylene.[99] In HEPES buffer (10 mM, pH = 7.4) and excitation wavelength of 530 ± 5 nm, the addition of Cd^{2+} rapidly turned on the fluorescence of probe **91**, and the fluorescence emission intensity increased with the concentration of Cd^{2+} ion from 0 to 300 μM. In addition, since two pyridine and chelidamic acid moieties of probe **91** chelating Cd^{2+} shortens the effective conjugate chain length of probe **91**, different amounts of Cd^{2+} caused the colorimetric change of probe **91** from blue to red(-violet). Probe **91** binds to Cd^{2+} in a stoichiometric ratio of 2 : 1, and the LOD for Cd^{2+} is as low as 1.85×10^{-5} M.

M. Y. Tang *et al.* reported probe **92** of nitrogen sulfur doped carbon dots (N&S CDs) with high water solubility, selectivity, sensitivity and stability to Cd^{2+}.[100] Using triethylenetetramine (TETA) and 2-mercaptothiazoline (2-MT) as raw materials can significantly improve the quantum yield of CDs, and they have rich sulfhydryl and amino groups that can provide more opportunities for application implementation. When excited at 340 nm, the probe **92** can quickly (2 min) recognize Cd^{2+} in ultrapure water and real water samples and quench the bright blue fluorescence at 459 nm. Because the fluorescence quenching of the probe caused by the potential aggregation of Cd^{2+} and sulfhydryl and amide groups on the surface of N&S CDs. Probe **92** has no obvious reaction with metal ions, biomolecules and anions other than Cd^{2+}, and the presence of other metal ions in the detection system also has no obvious interference with the detection of Cd^{2+}. The probe **92** can quantitatively detect the Cd^{2+} concentration of 0.02–1 μM, and the detection limit is 0.018 μM. In addition, the probe **92** not only has low toxicity and good cell permeability, but also remains stable in the pH range of 4–12 (the best detection pH is 9).

C. Wei's team reported the first quaternary QDs (Zn–Ag–In–S QDs) probe **93** based on aggregation-induced emission enhancement (AIEE) mechanism.[91] Under the phosphate buffer solution (pH = 7.4) and the excitation wavelength of 360 nm, the probe **93** reacts with metal ions for 20 min before fluorescence detection. Since L-cysteine is used as a stabilizer and ligand of Zn–Ag–In–S QDs, it can coordinate with Cd^{2+} through thiol groups, resulting in enhanced fluorescence emission and blue-shifted the emission peak of probe **93**, and formed macroscopic floc in the presence of high concentration of Cd^{2+}. Because the coordination of thiol groups with Cd^{2+} weakens the electrostatic repulsion between QDs, forms micro-heterojunctions and passivates surface defects, so the probe **93** shows enhanced fluorescence. In addition, Cd^{2+} may diffuse into Zn–Ag–In–S QDs to widen the band gap, and the emission peak of probe **93** is blue shifted at 520 nm. Probe **93** can quantitatively detect Cd^{2+} (25 μM to 2 mM), and the detection limit is 1.56 μM. In addition, the presence of Pb^{2+}, Hg^{2+} and

Cu^{2+} can also cause the fluorescence change (quenching the fluorescence) of probe **93**. The effects of Pb^{2+} and Hg^{2+} are eliminated by adding ammonium fluoride and thiosemicarbazide as masking agents, and the effects of Cu^{2+} are decreased by chelating Cu^{2+} with L-cysteine in advance.

In 2020, according to the hard-soft acid base (HSAB) principle, the soft donor site can react with soft toxic metals. M. Arnab's team constructed a three-dimensional columnar layered Zn-MOF sensor **94** using bis(pyridin-4-ylmethylene) benzene-1,4-diamine (as the Cd^{2+} ligand), thiophene-2,5-dicarboxylic acid and $Zn(NO_3)_2$.[101] When Cd^{2+} was added to the CH_3CN solution of sensor **94**, it can be observed by the naked eye that the color immediately changes from a very faint green colour to a deep orange. Upon the excitation at 330 nm, the addition of Cd^{2+} combined the emission peaks of sensor **94** at 390 nm and 468 nm into one emission peak at 446 nm, and the blue emission peak moved to 408 nm with the increase of the amount of Cd^{2+}. In addition, the addition of Cd^{2+} enhanced the fluorescence lifetime and fluorescence intensity (408 nm) of sensor **94**. The detection limit of sensor **94** for Cd^{2+} is 0.132 μM. Moreover, by repeatedly cleaning the sensor **94** that has been used for Cd^{2+} detection, the reversibility of the sensor can be realized.

Z. Q. Zhou's team reported a fluorescent probe **95**, which turns on fluorescence to identify Cd^{2+} by replacing Mn^{2+} near the surface of Mn:ZnSe QDs with Cd^{2+}.[102] The doping of Mn^{2+} near the QD surface reduces the fluorescence intensity of probe **95**. Due to the similar ion radius between Cd^{2+} and Zn^{2+}, the external Mn^{2+} is replaced by Cd^{2+}, resulting in the probe **95** emitting strong orange fluorescence and the fluorescence intensity increases by 20 times. The researchers optimized the detection conditions of probe **95** for the detection of Cd^{2+} in aqueous medium, such as the optimal concentration of probe **95** is 0.01 mg mL^{-1}, the optimal pH is 7 (higher pH is conducive to the deprotonation and electronegativity of MPA, so as to enhance the electrostatic attraction with Cd^{2+}) and the optimal reaction time is 15 min. Strong orange fluorescence of probe **95** was observed only when incubated with Cd^{2+}. Under the excitation of 367 nm light, the fluorescence intensity at 600 nm is linear with Cd^{2+} concentration (0.02–60 μM), and Cd^{2+} as low as 18 nM can be detected.

P. Subhash Chandra *et al.* synthesized carbon dots sensor **96** using curry leaves as carbon source for the first time.[103] Since the amine group in probe **96** provides donate an electron pair to excited state vacant orbital of the Cd^{2+} to form ligand-to-metal charge transfer (LMCT) process, the sensor recognizes Cd^{2+} by fluorescence off. The addition of Cd^{2+} not only reduced the fluorescence intensity and fluorescence lifetime of probe **96**, but also shifted its absorption peak and emission peak to lower wavelengths by about 10 nm. At the excitation wavelength of 390 nm, Cd^{2+} was added to the aqueous solution of probe **96** for 15 min, and the fluorescence emission of probe **96** at 450 nm was detected. The fluorescence intensity ratio at 450 nm before and after adding Cd^{2+} to probe **96** has a good linear relationship with the concentration of Cd^{2+} (0.01–8 M), and Cd^{2+} as low as 0.29 nM can be detected quantitatively. Other metal ions do not affect the fluorescence emission of probe **96** or the fluorescence

response of probe **96** to Cd^{2+}. However, due to the presence of phenol (–OH) and carbonyl groups (C=O, positive charge carrier) on the surface of the probe **96**, the fluorescence properties of the probe are pH dependent.

T. Alizadeh's team synthesized a fluorescent imprinted polymer probe **97** by a combination of hydrophilic functional monomers and hydrophobic ligands.[104] The luminescent complexing agent 5-((3hydroxynaphthalen-2-yl)methylene) pyrimidine-2,4,6(1,3,5)-trione (HMPT) forms a stable complex with Cd^{2+}, then the mixture of acryl amide, vinyl benzene and ethylene glycol dimethacrylate are added for copolymerization, and finally Cd^{2+} is extracted from the polymer, resulting in a cavity, which can be selectively recombined with Cd^{2+}. At the excitation wavelength of 365 nm, Cd^{2+} was added to turn on the high-intensity red fluorescence of probe **97**, and the emission peak blue-shifted from 440 nm to 502 nm. After the probe **97** reacted with Cd^{2+} for 20 min, the emission intensity at 502 nm had a good correlation with the concentration of Cd^{2+} (10 to 0.05 mM). The limit of detection (LOD) and limit of quantification (LOQ) of probe **97** for Cd^{2+} were 12.3 and 41 nM, respectively. Probe **97** not only has high selectivity, but also has low cytotoxicity. It also can be used as a fluorescent probe for the detection of Cd^{2+} in living cells.

In 2021, W. T. Li *et al.* reported a dual-emission ratiometric fluorescence probe **98**, in which silicon oxide-coated copper nanoclusters (CuNCs@SiO$_2$) as signal reference and cadmium telluride quantum dots (CdTe QDs) as signal response.[105] Since SiO$_2$ coating prevents the reaction of CuNCs with other substances, it is ensured that CuNCs@SiO$_2$ can provide a stable and reliable reference signal. In addition, based on the strong affinity of the two nitrogen atoms of 1,10-phenanthroline (Phen) for Cd in CdTe QDs, the researchers prepared CdTe QDs–Phen complex probe. Due to the photo-induced hole transfer (PHT) between CdTe QDs and Phen, the fluorescence of CdTe QDs–Phen complex probe is weak. After adding Cd^{2+}, Phen separated from CdTe QDs–Phen complex and formed $[Cd(Phen)_2(H_2O)_2]^{2+}$ and CdTe QDs, so the fluorescence intensity of CdTe QDs recovered. Under the excitation of 365 nm light, the characteristic fluorescence emission peaks of CuNCs@SiO$_2$ and CdTe QDs are well separated at 440 nm and 580 nm respectively, and the addition of Cd^{2+} only increases the fluorescence of CdTe QDs at 580 nm. Therefore, the Cd^{2+} content can be quantitatively analyzed according to the fluorescence intensity ratio (I_{580}/I_{436}) of probe **98** between 580 nm and 436 nm. The ratio fluorescent probe **98** can be sensitive with a detection limit of 1.1 μg L^{-1} (2.75 μg kg^{-1}) in a detection time of 6 min, and the detection can eliminate background interference, with high sensitivity and accuracy. In addition, the fluorescent color captured by the smartphone camera can be converted into digital values representing red, green and blue (RGB) color modes through the Color Picker app, and Cd^{2+} can be quantitatively analyzed through the ratio (G/R) of green (G) and red channels (R).

Table 8 shows the spectroscopic and analytical parameters of Cd^{2+} recognition based on nanosensors. Sensors based on MOF, QDs, nanoclusters and nanoparticles have achieved good development in recent years. For example, probe with enhanced

Table 8 Spectroscopic and analytical parameters of the nanosensor based Cd^{2+} fluorescent and colorimetric probes

Probe	Luminous structure	Solvent	Excitation wavelength (nm)	Emission wavelength (nm) λ_{em_0}–λ_{em}	Detection limit (nM)	Interfering ion(s)	Ref.
84	Ag$_2$S QDs	H$_2$O	480 (250–910)	1100	546	Zn^{2+}	93
85	Zr-MOF	H$_2$O	342	486	336	Fe^{3+}, Zn^{2+}	94
86	CdTe NPs	H$_2$O	328	468	130	Ag$^+$, Cu^{2+}	92
87	Eu-MOF	H$_2$O	324	613	1000	Mn^{2+}	95
88	CDs	H$_2$O	390	455	15	—	96
89	Zn-MOF	H$_2$O	333	529	1.19 µg mL^{-1}	Cu^{2+}, Mn^{2+}, Ni^{2+}, Co^{2+}	97
90	Au@g-CNQDs	H$_2$O	—	—	10	—	98
91	Polydiacetylene	H$_2$O	530	About 625	18 500	—	99
92	N&S CDs	H$_2$O	340	459	18	—	100
93	Zn–Ag–In–S QDs	H$_2$O	360	520	1560	Pb^{2+}, Hg^{2+}, Cu^{2+}	91
94	Zn-MOF	CH$_3$CN	330	390 and 468–446 -408	132	—	101
95	Mn:ZnSe QDs	H$_2$O	367	600	18	—	102
96	CDs	H$_2$O	390	450	0.29		103
97	Imprinted polymer	CH$_3$CN	365	440–502	12.3 (LOQ = 41)	—	104
98	CuNCs@SiO$_2$; CdTe QDs	H$_2$O	365	580 and 436	1.1 µg L^{-1}	—	105

near-infrared fluorescence emission are reported for the first time, AIE sensor based on quaternary quantum dots are reported for the first time, and quantum dot probe are synthesized using biomass as carbon source, *etc.* These nanosensors have good water solubility, but their selectivity, sensitivity, anti-interference ability and practicability (such as pH and response time) still need to be improved. These nanosensors can identify Cd^{2+} ions by chemical etching reaction, displacement reaction, cavity-imprinting, chelation passivation on the surface of nanoparticles and other methods. Researchers can design and improve the performances of nanosensors based on these mechanisms. In addition, the MOF sensor **85** based on C=N recognition of Cd^{2+}, the quaternary quantum dot sensor **93** synthesized with cysteine as the ligand of Cd^{2+}, and the ratiometric sensor **98** with 1,10-phenanthroline chelating Cd^{2+} to restore CdTe fluorescence. These reaction sites are similar to the design of small organic molecules sensors. Therefore, the idea of constructing and improving nanosensors can also be obtained based on the research results of small organic molecules probes in Cd^{2+} recognition.

10. Conclusions and outlooks

In this paper, we summarized the reports of Cd^{2+} fluorescent and colorimetric probes with different fluorophores since 2017, and found that there are still some problems to be solved in the practical application of Cd^{2+} fluorescent sensors. For example, the specific selectivity and anti-interference ability of most probes remain poor, which greatly affect the qualitative and quantitative detection of Cd^{2+} in complex environment. Secondly, the water solubility of many probes are poor, which inevitably result in addition of organic solvent into the detection medium and then pollution formation. Thirdly, the detection sensitivity of some probes are not enough to meet the maximum allowable concentration of Cd^{2+} in drinking water stipulated by WHO. Fourthly, few of the probes can realize near-infrared recognition of Cd^{2+}, and most of the probes only

identify Cd^{2+} in the blue and green light regions, which are easily interfered by the background fluorescence of biological samples and limits their application in biological system.

Therefore, the design and development of Cd^{2+} fluorescent probes in the future, on the one hand, need to discover and optimize the novel recognition groups with high selectivity, sensitivity and water solubility. On the other hand, overall consideration of the economy of raw materials, the simplicity of preparation, the practicability and feasibility of the probes, should be paid more attention. Finally and most importantly, the recognition pattern and mechanism of the probes should be elucidated clearly. Only in this way can we effectively perform the molecular structure design and find the lead compound with high performance.

Conflicts of interest

There are no conflicts to declare.

Acknowledgements

Notes and references

1 Y. Mikata, A. Kizu, K. Nozaki, H. Konno, H. Ono, S. Mizutani and S. Sato, *Inorg. Chem.*, 2017, **56**, 7404–7415.
2 C. Kumari, D. Sain, A. Kumar, S. Debnath, P. Saha and S. Dey, *Dalton Trans.*, 2017, **46**, 2524–2531.
3 K. Krishnaveni, M. Iniya, D. Jeyanthi, A. Siva and D. Chellappa, *Spectrochim. Acta, Part A*, 2018, **205**, 557–567.
4 J. Li, Y. H. Chen, T. T. Chen, J. Qiang, Z. J. Zhang, T. W. Wei, W. Zhang, F. Wang and X. Q. Chen, *Sens. Actuators, B*, 2018, **268**, 446–455.

5 J. Hao, X.-Y. Li, Y. Zhang and W.-K. Dong, *Materials*, 2018, **11**, 523.

6 P. G. Mahajan, N. C. Dige, B. D. Vanjare, E. Kamaraj, S. Y. Seo and K. H. Lee, *J. Photochem. Photobiol., A*, 2019, **385**, 112089.

7 Y. Zhang, X. F. Guo, M. M. Zheng, R. Yang, H. M. Yang, L. H. Jia and M. M. Yang, *Org. Biomol. Chem.*, 2017, **15**, 2211–2216.

8 W. Su, S. Z. Yuan and E. J. Wang, *J. Fluoresc.*, 2017, **27**, 1871–1875.

9 Y. P. Dai, K. Yao, J. X. Fu, K. Xue, L. Yang and K. X. Xu, *Sens. Actuators, B*, 2017, **251**, 877–884.

10 N. Behera and V. Manivannan, *J. Photochem. Photobiol., A*, 2018, **353**, 77–85.

11 X. Y. Liu, P. Wang, J. X. Fu, K. Yao, K. Xue and K. X. Xu, *J. Lumin.*, 2017, **186**, 16–22.

12 S. Chithiraikumar, C. Balakrishnan and M. A. Neelakantan, *Sens. Actuators, B*, 2017, **249**, 235–245.

13 R. Purkait, S. Dey and C. Sinhaa, *New J. Chem.*, 2018, **42**, 16653–16665.

14 J. K. Xiong, K. R. Wang, K. X. Wang, T. L. Han, H. Y. Zhu, R. X. Rong, Z. R. Cao and X. L. Li, *Sens. Actuators, B*, 2019, **297**, 126802.

15 L. Lvova, F. Caroleo, A. Garau, V. Lippolis, L. Giorgi, V. Fusi, N. Zaccheroni, M. Lombardo, L. Prodi, C. Di Natale and R. Paolesse, *Front. Chem.*, 2018, **6**, 258.

16 A. Maity, U. Ghosh, D. Giri, D. Mukherjee, T. K. Maiti and S. K. Patra, *Dalton Trans.*, 2019, **48**, 2108–2117.

17 J. Q. Sun, B. F. Ye, G. M. Xia and H. M. Wang, *Sens. Actuators, B*, 2017, **249**, 386–394.

18 Z. Wang, S. Q. Cui, S. Y. Qiu and S. Z. Pu, *J. Photochem. Photobiol., A*, 2018, **367**, 212–218.

19 D. D. Cheng, X. L. Liu, Y. D. Xie, H. T. Lv, Z. Q. Wang, H. Z. Yang, A. X. Han, X. M. Yang and L. Zang, *Sensors*, 2017, **17**, 2517.

20 T. Nemeth, T. Toth, G. T. Balogh and P. Huszthy, *Period. Polytech., Chem. Eng.*, 2017, **61**, 249–257.

21 D. B. Zhang, S. Y. Li, R. M. Lu, G. Liu and S. Z. Pu, *Dyes Pigments*, 2017, **146**, 305–315.

22 X. X. Zhang, R. J. Wang, C. B. Fan, G. Liu and S. Z. Pu, *Dyes Pigments*, 2017, **139**, 208–217.

23 M. Ghosh, S. Ta, M. Banerjee, M. Mahiuddin and D. Das, *ACS Omega*, 2018, **3**, 4262–4275.

24 R. Diana, U. Caruso, S. Concilio, S. Piotto, A. Tuzi and B. Panunzi, *Dyes Pigments*, 2018, **155**, 249–257.

25 H. L. Liu, S. Q. Cui, F. Shi and S. Z. Pu, *Dyes Pigments*, 2019, **161**, 34–43.

26 T. H. Liu, K. Liu, J. L. Zhang and Z. L. Wang, *ChemistrySelect*, 2018, **3**, 5559–5565.

27 Y. Y. Zhang, X. Z. Chen, X. Y. Liu, M. Wang, J. J. Liu, G. Gao, X. Y. Zhang, R. Z. Sun, S. C. Hou and H. M. Wang, *Sens. Actuators, B*, 2018, **273**, 1077–1084.

28 Z. Wang, S. Q. Cui, S. Y. Qiu and S. Z. Pu, *Tetrahedron*, 2018, **74**, 7431–7437.

29 M. Vera, H. S. Ortega, M. Inoue and L. Machi, *Supramol. Chem.*, 2019, **31**, 336–348.

30 P. Kaur, B. Lal, N. Kaur, G. Singh, A. Singh, G. Kaur and J. Singh, *J. Photochem. Photobiol., A*, 2019, **382**, 111847.

31 M. Banerjee, M. Ghosh, S. Ta, J. Das and D. Das, *J. Photochem. Photobiol., A*, 2019, **377**, 286–297.

32 M. Maniyazagan, R. Mariadasse, J. Jeyakanthan, N. K. Lokanath, S. Naveen, K. Premkumar, P. Muthuraja, P. Manisankar and T. Stalin, *Sens. Actuators, B*, 2017, **238**, 565–577.

33 X. J. Wan, H. Q. Ke, J. N. Tang and G. H. Yang, *Talanta*, 2019, **199**, 8–13.

34 Y. F. Tang, Y. Huang, Y. H. Chen, L. X. Lu, C. Wang, T. M. Sun, M. Wang, G. H. Zhu, Y. Yang, L. Zhang and J. L. Zhu, *Spectrochim. Acta, Part A*, 2019, **218**, 359–365.

35 J. Jia, X. Tang, Y. He, M. Zhang and G. Xing, *Chin. J. Org. Chem.*, 2012, **32**, 1803–1811.

36 S. Y. Chen, Z. Li, K. Li and X. Q. Yu, *Coord. Chem. Rev.*, 2021, **429**, 20.

37 Y. Mikat, M. Kaneda, H. Konno, A. Matsumoto, S. Sato, M. Kawamura and S. Iwatsuki, *Dalton Trans.*, 2019, **48**, 3840–3852.

38 Y. Mikata, M. Kaneda, M. Tanaka, S. Iwatsuki, H. Konno and A. Matsumoto, *Eur. J. Inorg. Chem.*, 2020, **2020**, 757–763.

39 Y. Zhang, X. F. Guo, L. B. Zheng and L. H. Jia, *J. Lumin.*, 2017, **188**, 283–288.

40 X. H. Ding, F. F. Zhang, Y. J. Bai, J. X. Zhao, X. Chen, M. Ge and W. Sun, *Tetrahedron Lett.*, 2017, **58**, 3868–3874.

41 H. H. Song and Z. Zhang, *Dyes Pigments*, 2019, **165**, 172–181.

42 Z. N. Lu, L. Wang, X. Zhang and Z. J. Zhu, *Spectrochim. Acta, Part A*, 2019, **213**, 57–63.

43 K. Aich, S. Das, S. Gharami, L. Patra and T. K. Mondal, *ChemistrySelect*, 2019, **4**, 8068–8073.

44 S. Nazerdeylami, J. B. Ghasemi, A. Amiri, G. M. Ziarani and A. Badiei, *Methods Appl. Fluoresc.*, 2020, **8**, 025009.

45 S. L. Li, D. L. Cao, W. B. Ma, Z. Y. Hu, X. J. Meng, Z. C. Li, C. C. Yuan, T. Zhou and X. H. Han, *RSC Adv.*, 2020, **10**, 18434–18439.

46 Y. Xiao, J. Ma, D. H. Li, L. Liu and H. L. Wang, *J. Photochem. Photobiol., A*, 2020, **399**, 112613.

47 A. Garau, M. C. Aragoni, M. Arca, A. Bencini, A. J. Blake, C. Caltagirone, C. Giorgi, V. Lippolis and M. A. Scorciapino, *Chempluschem*, 2020, **85**, 1789–1799.

48 J. Han, X. Tang, Y. Wang, R. J. Liu, L. Wang and L. Ni, *Spectrochim. Acta, Part A*, 2018, **205**, 597–602.

49 S. Zehra, R. A. Khan, A. Alsalme and S. Tabassum, *J. Fluoresc.*, 2019, **29**, 1029–1037.

50 A. K. Shaily and N. Ahmed, *New J. Chem.*, 2017, **41**, 14746–14753.

51 S. Paul and P. Banerjee, *Sens. Actuators, B*, 2021, **329**, 129172.

52 P. Sakthivel, K. Sekar, G. Sivaraman and S. Singaravadivel, *J. Fluoresc.*, 2017, **27**, 1109–1115.

53 P. Wang, L. P. Duan and Y. W. Liao, *Microchem. J.*, 2019, **146**, 818–827.

54 P. Wang, K. Chen and Y. S. Ge, *J. Lumin.*, 2019, **208**, 495–501.

55 P. Wang, D. G. Zhou and B. Chen, *Spectrochim. Acta, Part A*, 2019, **207**, 276–283.

56 P. Wang, Y. An and Y. W. Liao, *Spectrochim. Acta, Part A*, 2019, **216**, 61–68.

57 P. Wang, J. Wu and C. H. Zhao, *Spectrochim. Acta, Part A*, 2020, **226**, 117600.

58 S. Guo, G. Liu, C. Fan and S. Pu, *RSC Adv.*, 2018, **8**, 22786–22798.

59 J. F. Lv, G. Liu, C. B. Fan and S. Z. Pu, *Spectrochim. Acta, Part A*, 2020, **227**, 117581.

60 W. B. Huang, W. Gu, H. X. Huang, J. B. Wang, W. X. Shen, Y. Y. Lv and J. Shen, *Dyes Pigments*, 2017, **143**, 427–435.

61 N. A. Bumagina, E. V. Antina and D. I. Sozonov, *J. Lumin.*, 2017, **183**, 315–321.

62 V. Tekuri and D. R. Trivedi, *Anal. Chim. Acta*, 2017, **972**, 81–93.

63 Y. Tang, H. Liu, G. Jiang and Z. Gu, *J. Appl. Spectrosc.*, 2017, **84**, 911–914.

64 S. Poomalai, A. K. Padinjareveetil, S. Ramasamy, T. S. Govindaraj, M. S. Paulraj and I. Enoch, *Luminescence*, 2017, **32**, 1405–1410.

65 W. H. Hsieh, C.-F. Wan, D.-J. Liao and A.-T. Wu, *Tetrahedron Lett.*, 2012, **53**, 5848–5851.

66 P. Kaur, J. Singh, R. Singh, V. Kaur and D. Talwar, *Polyhedron*, 2017, **125**, 230–237.

67 B. K. Momidi, V. Tekuri and D. R. Trivedi, *Spectrochim. Acta, Part A*, 2017, **180**, 175–182.

68 V. Kumar, P. Kumar and R. Gupta, *RSC Adv.*, 2017, **7**, 23127–23135.

69 M. Findik, A. Ucar, H. Bingol, E. Guler and E. Ozcan, *Res. Chem. Intermed.*, 2017, **43**, 401–412.

70 Y. Y. Zhang, X. Z. Chen, J. J. Liu, G. Gao, X. Y. Zhang, S. C. Hou and H. M. Wang, *New J. Chem.*, 2018, **42**, 19245–19251.

71 M. Formica, G. Ambrosi, V. Fusi, L. Giorgi, M. Arca, A. Garau, A. Pintus and V. Lippolis, *New J. Chem.*, 2018, **42**, 7869–7883.

72 P. Ravichandiran, A. Boguszewska-Czubara, M. Maslyk, A. P. Bella, P. M. Johnson, S. A. Subramaniyan, K. S. Shim and D. J. Yoo, *Dyes Pigments*, 2020, **172**, 107828.

73 M. Das and M. Sarkar, *ChemistrySelect*, 2019, **4**, 681–692.

74 M.-X. Huang, C.-H. Lv, Q.-D. Huang, J.-P. Lai and H. Sun, *RSC Adv.*, 2019, **9**, 36011–36019.

75 W. X. Lin, X. C. Xie, Y. J. Wang and J. J. Chen, *Z. Anorg. Allg. Chem.*, 2019, **645**, 645–648.

76 P. P. Namitha, A. Saji, S. Francis and L. Rajith, *J. Fluoresc.*, 2020, **30**, 527–535.

77 P. Liu, J. Liu, F. Yao, X. M. Zhan and X. P. Qi, *J. Photochem. Photobiol., B*, 2020, **202**, 111717.

78 B. Jana, S. Maity, A. Mondal and J. Ganguly, *J. Lumin.*, 2020, **222**, 117128.

79 E. K. Inal, *J. Fluoresc.*, 2020, **30**, 891–900.

80 S. G. J. Andrews, S. B. J. Silviya, D. Jeyanthi, E. S. Devi, J. W. Jebaraj and C. Balakrishnan, *Analyst*, 2020, **145**, 4576–4586.

81 Y. F. Zhang, L. Chen, J. Yang, Y. R. Zhang and M. S. Yuan, *Spectrochim. Acta, Part A*, 2020, **232**, 118163.

82 F. D. Carlos, L. A. da Silva, C. Zanlorenzi and F. S. Nunes, *Inorg. Chim. Acta*, 2020, **508**, 119634.

83 S. Park, H. Lee, Y. Yi, M. H. Lim and C. Kim, *Inorg. Chim. Acta*, 2020, **513**, 119936.

84 P. S. Kumar and K. P. Elango, *Spectrochim. Acta, Part A*, 2020, **241**, 118610.

85 Z. Aydin and M. Keles, *Turk. J. Chem.*, 2020, **44**, 791–804.

86 J. J. Celestina, P. Tharmaraj and C. D. Sheela, *Opt. Mater.*, 2020, **109**, 110176.

87 P. Lasitha, S. Dasgupta and G. N. Patwari, *ChemPhysChem*, 2020, **21**, 1564–1570.

88 M. Muddassir, A. Alarifi, M. Afzal, K. A. Alshali, N. A. Y. Abduh and A. Beagan, *RSC Adv.*, 2020, **10**, 42137–42146.

89 S. Dey, R. Purkait, D. Mallick and C. Sinha, *ChemistrySelect*, 2020, **5**, 8274–8283.

90 D. Yue, X. Zhang, Y. Tan, Z. Wang and Y. Zhang, *J. Lumin.*, 2020, **228**, 117618.

91 C. Wei, X. Wei, Z. Hu, D. Yang, S. Mei, G. Zhang, D. Su, W. Zhang and R. Guo, *Anal. Methods*, 2019, **11**, 2559–2564.

92 L. Li, L. Liao, Y. Ding and H. Zeng, *RSC Adv.*, 2017, **7**, 10361–10368.

93 Q. Wu, M. Zhou, J. Shi, Q. Li, M. Yang and Z. Zhang, *Anal. Chem.*, 2017, **89**, 6616–6623.

94 J. Wang, T. Xia, X. Zhang, Q. Zhang, Y. Cui, Y. Yang and G. Qian, *RSC Adv.*, 2017, **7**, 54892–54897.

95 Y. Yang, L. Chen, F. Jiang, X. Wan, M. Yu, Z. Cao, T. Jing and M. Hong, *J. Mater. Chem. C*, 2017, **5**, 4511–4519.

96 D. Gu, L. Hong, L. Zhang, H. Liu and S. Shang, *J. Photochem. Photobiol., B*, 2018, **186**, 144–151.

97 Y. Pan, J. Wang, X. Guo, X. Liu, X. Tang and H. Zhang, *J. Colloid Interface Sci.*, 2018, **513**, 418–426.

98 Z. Zhang, Z. Zhang, H. Liu, X. Mao, W. Liu, S. Zhang, Z. Nie and X. Lu, *Biosens. Bioelectron.*, 2018, **103**, 87–93.

99 P. Thanh Chung, Y. K. Kim, J. B. Park, S. Jeon, J. Ahn, Y. Yim, J. Yoon and S. Lee, *ChemPhotoChem*, 2019, **3**, 1133–1137.

100 M. Tang, X. Liu, N. Zhang, J. Pang, Y. Zou, F. Chai, H. Wu and L. Chen, *Anal. Methods*, 2019, **11**, 5214–5221.

101 A. Mandal, A. Adhikary, A. Sarkar and D. Das, *Inorg. Chem.*, 2020, **59**, 17758–17765.

102 Z.-Q. Zhou, L.-Y. Yang, Y.-P. Liao, H.-Y. Wu, X.-H. Zhou, S. Huang, Y. Liu and Q. Xiao, *Anal. Methods*, 2020, **12**, 552–556.

103 S. C. Pandey, A. Kumar and S. K. Sahu, *J. Photochem. Photobiol., A*, 2020, **400**, 112620.

104 T. Alizadeh, A. R. Sharifi and M. R. Ganjali, *RSC Adv.*, 2020, **10**, 4110–4117.

105 W. Li, X. Zhang, X. Hu, Y. Shi, Z. Li, X. Huang, W. Zhang, D. Zhang, X. Zou and J. Shi, *J. Hazard. Mater.*, 2021, **408**, 124872.